RESEARCH PAPER

The Cenomanian–Turonian transition in the carbonate platform facies of the Western Saharan Atlas (Rhoundjaïa Formation, Algeria)

Mustapha Benadla[1] · Matías Reolid[2] · Abbas Marok[1] · Nezha El Kamali[3]

Abstract

Microfacies, fossil macroinvertebrates and microfossil assemblages (foraminifera and ostracods) and $\delta^{13}C$ from the Rhoundjaïa Formation (Ksour Mountains, Western Saharan Atlas, Algeria) were studied. During the Late Cenomanian–Early Turonian, the Ksour Basin was an isolated platform at mid to outer shelf depths. The neritic conditions were interrupted by pelagic conditions in transgressive intervals. This deepening of the palaeoenvironment is reflected by changes in the foraminiferal assemblages. The composition of benthic and planktic foraminiferal assemblages, characterized by low diversity and abundance of low oxygen tolerant species, reflects a carbonate platform with biotic stress conditions (oxygen and nutrient fluctuations and sea-level changes). Planktic foraminiferal assemblages are dominated by opportunists such as *Muricohedbergella* and *Planoheterohelix*, which colonized new ecospace on the shelf during the transgression. The Oceanic Anoxic Event 2 (OAE2) is not represented by organic rich facies but does coincide with the successive proliferation of different opportunist organisms such as microgastropods and small echinoid (hemiasterids) and the heterohelicid shift. The continuous presence of trace fossils (*Thalassinoides* and *Planolites*-like) and benthic macroinvertebrates allows us to exclude anoxic conditions during the *Whiteinella archaeocretacea* Zone. The proliferation of *Planoheterohelix* indicates the record of eutrophic conditions and the transition from oxygenated to poorly oxygenated waters during stratified open marine settings at the time of maximum flooding. The subsequent increase in thin-shelled bivalves and cytherellid ostracods would confirm the stress conditions at the time of the $\delta^{13}C$ isotopic excursion in the upper part of the *W. archaeocretacea* Zone. The Lower Turonian is represented by a shallowing upward trend in the Ksour Basin. Comparison of the taxonomic composition of the planktic foraminiferal assemblages (phenogram and class diagram) indicates the high degree of relationship of the Ksour Basin with the Northeast Sicily Basin, Central Tunisia Basin and Egypt. This work sheds light on the impact of the OAE2-related environmental perturbation in environments where anoxic conditions were not reached, as well as the response of the fossil assemblages to the biotic crisis.

Keywords Microfacies · Foraminifera · Ostracods · Opportunist · Biotic crisis · North Gondwana Palaeomargin

Resumen

Se han estudiado las microfacies, las asociaciones de macroinvertebrados fósiles y microfósiles (foraminíferos y ostrácodos) y el ^{13}C en la Formación Rhoundjaïa (Montes Ksour, Atlas Sahariano Occidental, Argelia). Durante el Cenomaniense superior-Turoniense temprano, la Cuenca de Ksour fue una plataforma relativamente aislada con unas características entre plataforma media y externa. Las condiciones neríticas cambiaron a condiciones pelágicas durante los intervalos transgresivos. La profundización de los paleoambientes queda registrada por cambios en las asociaciones de foraminíferos. La composición de las asociaciones de foraminíferos bentónicos y planctónicos caracterizada por baja diversidad y por la abundancia de species tolerantes de baja oxigenación, refleja una plataforma cabonatada con condiciones de estrés biológico (variaciones en el grado de oxigenación, contenido en nutrientes y nivel del mar). Las asociaciones de foraminíferos planctónicos están dominadas por oportunistas tales como *Muricohedbergella* y *Planoheterohelix*, que colonizaron el incremento de ecoespacio creado en la plataforma durante la transgresión. El evento anóxico oceánico 2 (Oceanic Anoxic Event 2, OAE2) no está representado por facies ricas en materia orgánica sino que coincide con la sucesivas etapas de proliferación de diferentes grupos de oportunistas como microgasterópodos y pequeños equinoideos (hemiastéridos) y la proliferación de heterohelícidos. El registro

continuado de trazas fósiles (*Thalassinoides* y posibles *Planolites*) y de macroinvertebrados bentónicos permite excluir la existencia de condiciones plenamente anóxicas durante la Zona de *Whiteinella archaeocretacea* Zone. La proliferación de *Planoheterohelix* indica el registro de condiciones eutróficas y y el empobrecimiento en oxígeno de las aguas, posiblemente relacionado con una estratificación en la columna de agua durante la fase de máxima inundación. El posterior incremento en pequeños bivalvos de concha fina (filamentos) y ostrácodos citherellidos confirmaría las condiciones de estrés ambiental al tiempo que se producíala excrusión isotópica del ^{13}C en la parte superior de la Zona de *Whiteinella archaeocretacea*. El Turoniense inferior está representado por una secuencia de somerización en la Cuenca de Ksour. La comparación de la composición taxonómica de las asociaciones de foraminíferos planctónicos (fenogramas y diagramas de clases) indica un alto grado de relación entre las asociaciones de la Cuenca de Ksour con el Noreste de la Cuenca de Sicilia, la Cuenca Central de Túnez y Egipto. Este trabajo muestra un ejemplo del impacto de las perturbaciones que acompañaron al OAE en ambientes donde no se desarrollaron condiciones anóxicas así como la respuesta de las asociaciones fósiles a esta crisis biológica.

1 Introduction

The Cenomanian–Turonian transition is related to a global oceanic anoxic event known as Oceanic Anoxic Event 2 (OAE2) (Schlanger and Jenkyns 1976; Arthur and Schlanger 1979; Jenkyns 1980; Jarvis et al. 1988; Robaszynski 1989; Erbacher and Thurow 1997; Friedrich et al. 2006; Turgeon and Creaser, 2008; Voigt et al. 2008; Gebhardt et al. 2010; Uchman et al. 2013; Elderbak et al. 2014; Reolid et al. 2015, 2016). This anoxic event is associated with climatic and palaeogeographic changes including greenhouse warming (e.g. Huber et al. 2002; Bornemann et al. 2008; Monteiro et al. 2012), a sea-level rise (Arthur et al. 1987; Jones and Jenkyns 2001; Smith et al. 2001; Lowery et al. 2017) and a global positive δ^{13}C excursion (Pratt and Threlkeld 1984; Hilbrecht and Hoefs 1986; Accarie et al. 1996; Keller et al. 2004; Tsikos et al. 2004; Prokoph et al. 2013). Scaife et al. (2017) propose a magmatic pulse at the onset of OAE2, probably related to the emplacement of a Large Igneous Province (LIP) in the Pacific Ocean (Caribbean LIP and Ontong Java LIP), Indian Ocean (Madagascar LIP) and/or the High Arctic.

The OAE2 constitutes an extinction episode for marine ecosystems and marks a decreased diversity of foraminifera, radiolarians and calcareous nannoplankton (Robaszynski and Caron 1995; Jarvis et al. 1988; Harries and Kauffman 1990; Harries 1993; Harries and Little 1999; Leckie et al. 2002; Caron et al. 2006; Pearce et al. 2009; Aguado et al. 2016), as well as a period of expansion and homogenization of ammonite fauna on the South Tethyan carbonate platforms (Meister et al. 1992; Courville et al. 1991, 1998; Courville 2007). The OAE2 is typically related to organic-rich facies, locally identified as black shales (Arthur and Schlanger 1979; Arthur et al. 1987; Jarvis et al. 1988; Robaszynski et al. 1993a, b; Rhalmi et al. 2000; Lüning et al. 2004; Ettachfini et al. 2005; Shahin 2007; Scopelliti et al. 2008; Pearce et al. 2009; Westermann et al. 2010; Robaszynski et al. 2010; Yilmaz et al. 2010; Hetzel et al.

2011; Pavlishina and Wagreich 2012; Reolid et al. 2015). Possible causes of the OAE2 are increased productivity, the shallowing of the oxygen minimum zone (OMZ) and water stagnation (Busson and Cornée 1996; Hardas and Mutterlose 2007; Jarvis et al. 2011; Ruault-Djerrab et al. 2014). Other models indicate that water stagnation is unlikely during OAE2 because a consistent flux of nutrients is required to sustain high productivity for ~ 500 kyr (Trabucho-Alexandre et al. 2010; Topper et al. 2011; Monteiro et al. 2012). The hypothesis of global tectonic pulses related to volcanism has also been put forward (Kuroda et al. 2007; Turgeon and Creaser 2008).

In the North Gondwana palaeomargin, the Cenomanian–Turonian transition as well as the related OAE2 have been studied previously in Morocco (Rhalmi et al. 2000; Andreu 2002; Meister and Rhalmi 2002; Gebhardt et al. 2004, 2010; Ettachfini and Andreu 2005; Ettachfini et al. 2005; Kolonic et al. 2005; Kunht et al. 2005; Jati et al. 2010; Lézin et al. 2012; Prauss 2012; Andreu et al. 2013; Aquit et al. 2013), in Tunisia (Robaszynski et al. 1990, 1993a, b, c, 2010; Accarie et al. 1996, 2000; Caron et al. 1999, 2006; Nederbragt and Fiorentino 1999; Amédro et al. 2005; Meister and Abdallah 2005; Soua et al. 2006, 2011; Zagrarni et al. 2008; Negra et al. 2011; Grosheny et al. 2013; Zaghbib-Turki and Soua 2013; Reolid et al. 2015; Aguado et al. 2016) and in Egypt (Lüning et al. 1998; Aly and Abdel-Gawad 2001; Bauer et al. 2002; Shahin 2007; Gertsch et al. 2008; Wanas 2008; Ismail et al. 2009; Nagm 2015; El-Sabbagh et al. 2011; Ayoub-Hannaa et al. 2013; Shahin and Elbaz 2013; Wilmsen and Nagm 2013). In Algeria, however, works on the Cenomanian–Turonian transition are comparatively scarce (Naili et al. 1995; Busson et al. 1999; Harket and Delfaud 2000; Grosheny et al. 2008, 2013; Chikhi-Aouimeur et al. 2010; Ruault-Djerrab et al. 2012, 2014; Benyoucef et al. 2017; Ferré et al. 2017; Zaoui et al. 2017).

The aim of this contribution is to characterize the Cenomanian–Turonian transition in view of a representative
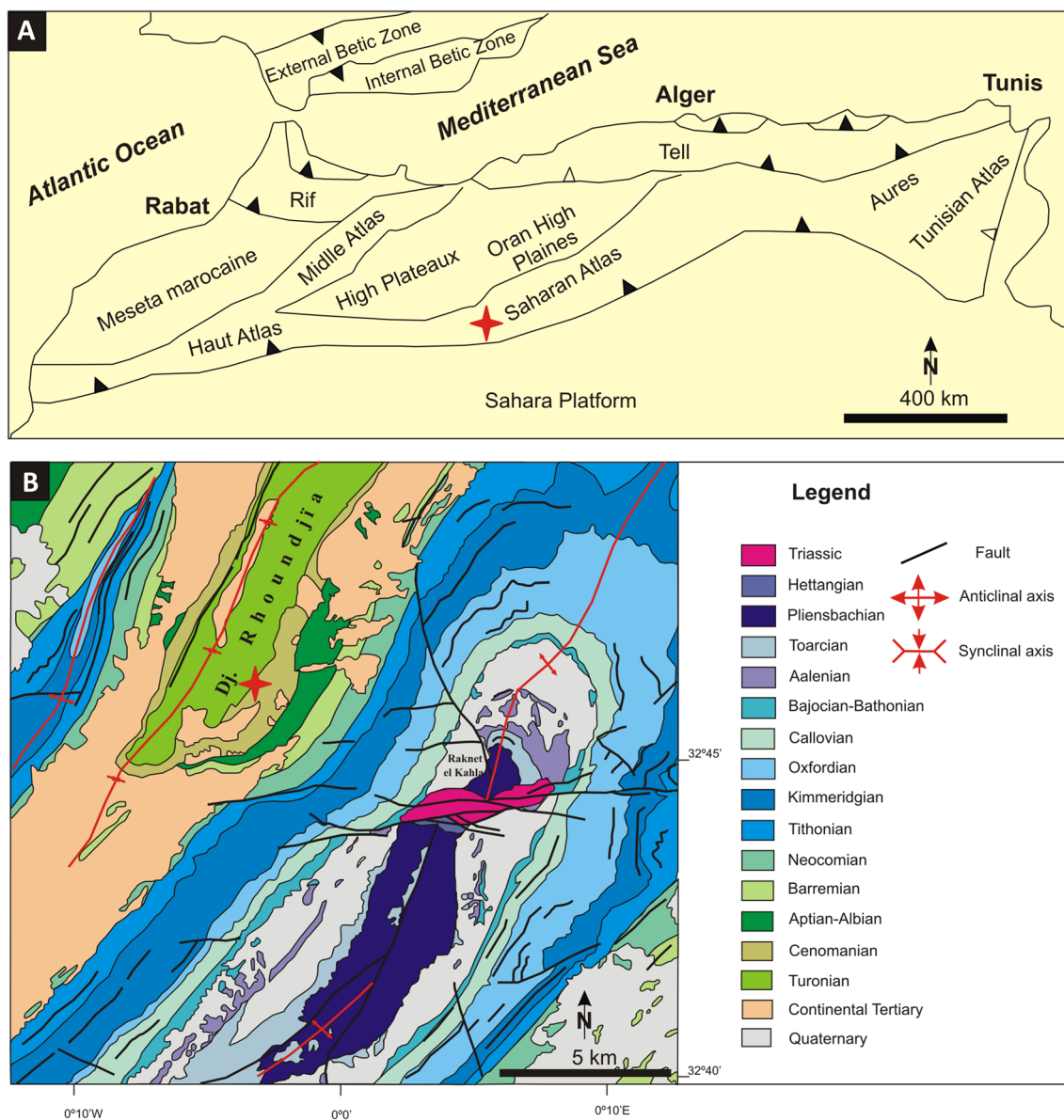
Fig. 1 Geological sketch. **a** Location map of the Western Saharan Atlas (Ksour Mountains). **b** Geological map of the area studied

well-exposed section from the Ksour Mountains in the western part of the Saharan Atlas. The studied area is relevant because it is located at the northern end of the Trans-Saharan-Seaway (Moody and Sutcliffe 1991). The Trans-Saharan-Seaway connected the Western Tethys and the South Atlantic in a period with limited palaeogeographic connections between South and North Atlantic (Scotese 2011). Unlike many other regional OAE2 sections, such as the Tunisian Oued Bahloul section, which were deposited in deeper environments, the studied Rhoundjaïa section never became anoxic during the Cenomanian–Turonian transition and it is thus an important record of the shallow water response to a major anoxic event. The work is focused on analyses of the microfacies, microfossil assemblages (foraminifera and

ostracods) and the C stable isotopes. The results lead us to interpret the prevailing palaeoenvironmental conditions as well as to infer the palaeogeographic evolution of this part of the carbonate platform in the context of the Maghrebian Atlasic System of the Gondwana Palaeomargin. In addition, the record of planktic foraminifera of the *W. archaeocretacea* Zone invites discussion about the connections between North Gondwanan basins and European basins.
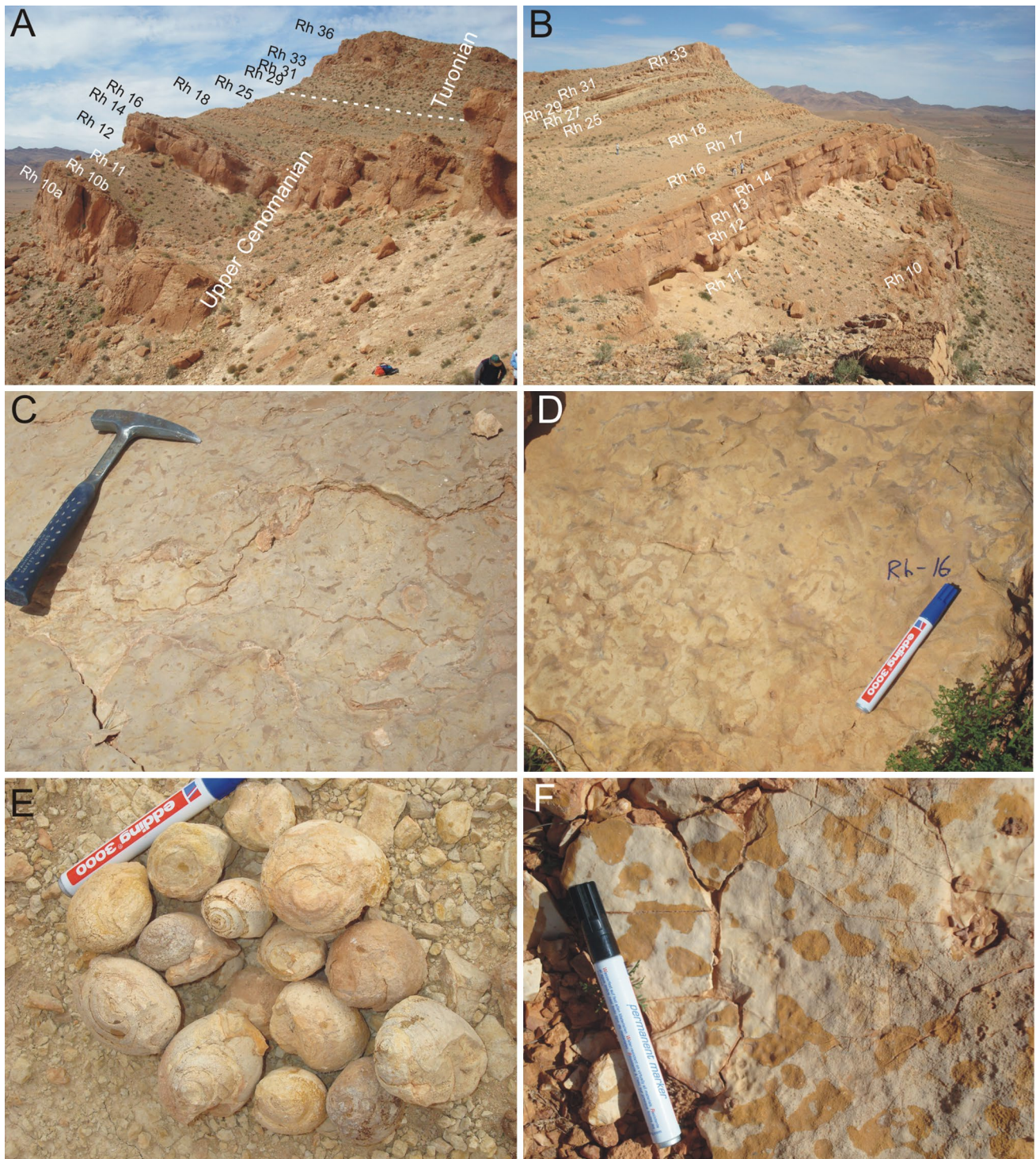
Fig. 2 Outcrop view and lithofacies. **a**, **b** Studied section with location of the Cenomanian/Turonian boundary. **c** Densely bioturbated limestone with *Thalassinoides* (bed RH 10a). **d** Densely bioturbated limestone with *Thalassinoides* (bed RH 16). **e** Abundant gastropods from RH 30′ (*Tylostoma*). **f** Large *Thalassinoides* in the lower Turonian commonly affected by recrystallization (bed RH 14)

2 Geographical and geological setting

The Ksour Mountains, located in the western part of the Saharan Atlas, are part of the Maghrebian Atlasic System (from West to East): High Atlas, of Morocco, Saharan Atlas, and the Aurès and Tunisian Atlas. The Ksour Mountains are limited to the North by the Oran High Plain, to the South by the Saharan Platform, to the East by the

Central Saharan Atlas (Djebel Amour) and to the West by the High Atlas of Morocco (Fig. 1a). This folded mountain belt developed in a subsiding intra-plate basin (Aït Ouali and Delfaud 1995). The folded mountain belt comprises of long, narrow anticlines composed of Triassic deposits (Germanic Facies) and Jurassic carbonates that constitute long and narrow anticlines. The anticlines are separated by large synclinals composed of well-preserved Cretaceous limestones and marls. The Cretaceous rocks are mainly constituted by siliciclastic successions (fluvio-deltaic deposits) of the Lower Cretaceous and marine carbonates of the Upper Cretaceous. During the Late Cenomanian a main transgression occurred in the Saharan Atlas (Busson et al. 1999; Grosheny et al. 2008, 2013). There are two main depositional sequences in the Saharan Atlas: CI (Cenomanian–Turonian) and CII (Santonian–Maastrichtian) (Delfaud 1986; Harket and Delfaud 2000). The Cenomanian–Turonian deposits constitute the upper part of the Mesozoic folded succession.

The Rhoundjaïa section (RH) is located 60 km East of Aïn Séfra, close to the road to Aïn Ouarka (Fig. 1b). The 55.15 m-thick Rhoundjaïa Formation is well-exposed at a cliff (Fig. 2a, b) and overlying by the M'Daouer Formation (claystones, gypsum, limestones, and dolostones). The present research focuses mainly on the upper 32.3 m of the Rhoundjaïa Formation in order to study the Cenomanian–Turonian transition.

3 Materials and methods

Analyses of microfacies, microfossils and geochemistry were conducted across the upper Cenomanian–Lower Turonian at the Rhoundjäia section, mainly composed by limestones and marly interlayers. A total of 67 limestone samples were studied in thin section for microfacies analysis. Differentiation of microfacies and proportions of different bioclasts have been based on a detailed point-count using a two-dimensional grid with a fine mesh-light with 1.5-mm opening. Additionally, 10 samples from marly interlayers (500 g per sample) were washed in water on a stainless sieve column (250, 125 and 63 μm) and picked for retrieving microfossils (foraminifera and ostracods). In these samples, at least 200 microfossils were picked. The classification of microfossils is based on Bassoullet and Damotte (1969), Tronchetti and Grosheny (1991), Okosun (1992), Andreu et al. (2013) and Haynes et al. (2015). Gold-coated specimens of microfossils from sieved samples were analysed under scanning electron microscopy (SEM); images were produced with a Merlin Carl Zeiss SEM in the Centro de Instrumentación Científico-Técnica of the Universidad de Jaén.

The taxonomic composition of the planktic foraminiferal assemblages was compared with data from previous studies of North African basins, as well as from European basins. The software BG-Index 1.1 β (Escarguel 2001) was used to process data, and the Simpson Coefficient indicates the degree of relationship. The results are represented as phenograms transformed to Class Diagrams.

For $\delta^{13}C$ and $\delta^{18}O$ analyses, and after roasting, the 21 samples were reacted at 73 °C in an automated carbonate reaction system (Kiel-IV) coupled directly to the inlet of a Finnigan MAT 253 gas ratio mass spectrometer at the Laboratory of Stable Isotopes of the University of Michigan. Isotopic ratios were corrected for ^{17}O contribution and are reported in per mil notation relative to the VPDB standard. Values were calibrated using NBS 19 as the primary standard, and analytical precision was monitored by daily analyses of NBS-powered carbonate standards. The measured precision was maintained above 0.02‰ for $\delta^{13}C$ and $\delta^{18}O$.

4 Results

4.1 Lithofacies and microfacies

The studied interval comprises 56.2 m of limestones with some marly interlayers in the upper part of the section (Fig. 2). The lithostratigraphic succession is divided in six stratigraphic intervals:

- Stratigraphic interval I (RH 1 to RH 9, 7.2 m): massive limestones in an upward-thinning sequence. The lower part of the section begins with wackestone–packstones of ostracods and foraminifera (mainly miliolids and textulariids, Fig. 3a, b). They change to mudstones-wackestones of planktic foraminifera (Fig. 3c, d), though they are mainly unkeeled trochospiral forms with globular chambers —hedbergellids (mainly *Muricohedbergella delrioensis*). From bed RH 3 trochospiral forms with strongly keeled high (planoconvex shape) chambers are also recorded, corresponding to *Dicarinella* sp. The weakly keeled forms with high chambers would be *Helvetoglobotruncana praehelvetica*. Finally, less common forms are represented by trochospiral shells featuring keeled low chambers interpreted as *Rotalipora* spp.

- Stratigraphic interval II (RH 10 to RH 14, 16.7 m): massive limestones with abundant trace fossils (*Thalassinoides* and *Planolites*-like, Fig. 2c). They correspond to wackestone to packstones of bioclasts rich in echinoderms (echinoids and ophiuroids; ~10–20%), bivalves, gastropods, ostracods and agglutinated benthic foraminifera (Fig. 3e–h). The top of bed RH 10 presents a high concentration of bivalve shells (infaunal and epifaunal ones, such as ostreids and pectinids). Planktic foraminifera are very scarce. They newly appear at the top (RH 14), as unkeeled trochospiral forms with globular cham-
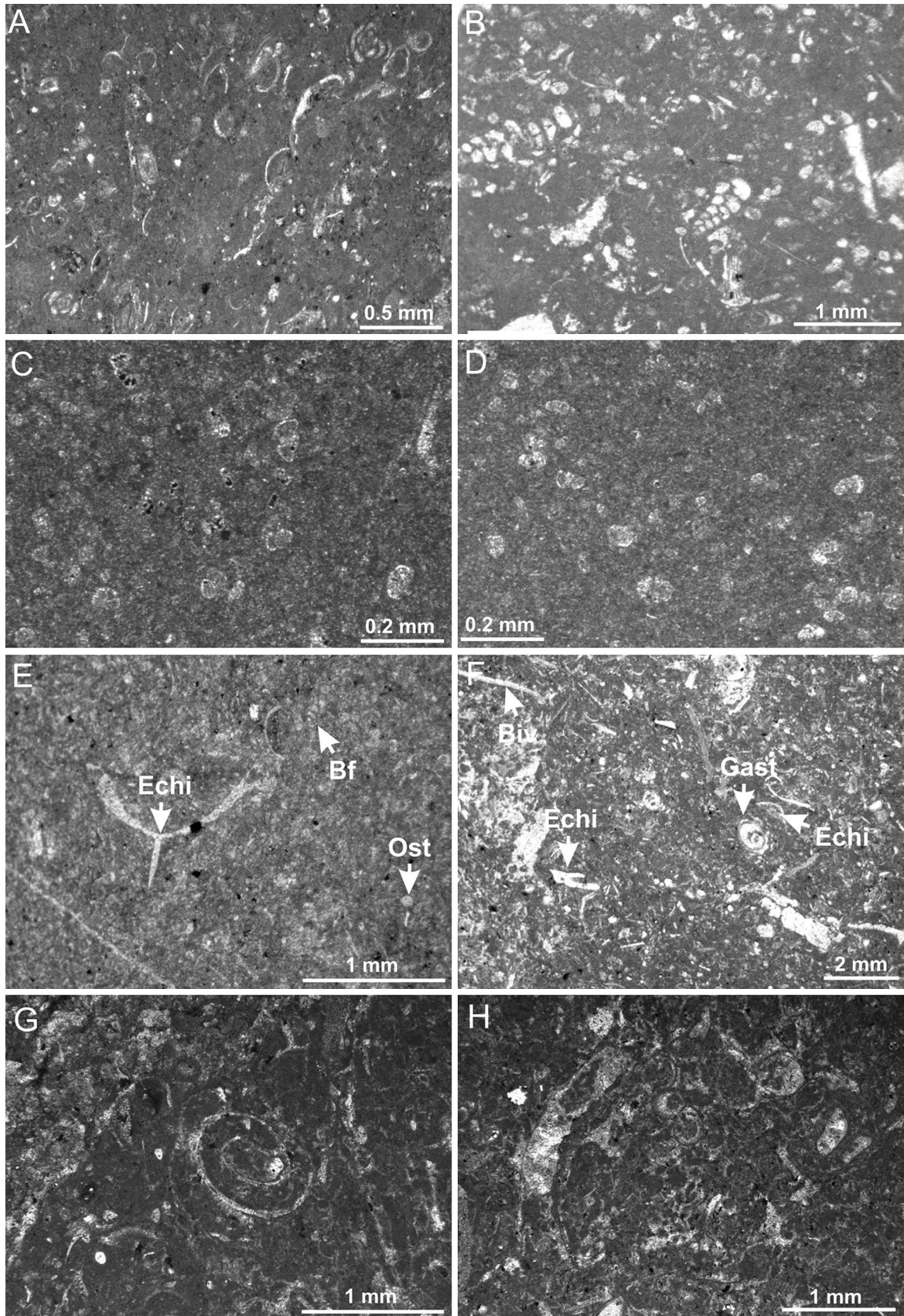
◀**Fig. 3** Microfacies rich in bioclasts. **a** Packstone of milolids and disarticulated ostracods from bed RH 1. **b** Biserial agglutinated foraminifera from bed RH 5. **c** Wackestone of planktic foraminifera from bed RH 6. **d** Wackestone of planktic foraminifera from bed RH 7. **e** Wackestone of bioclasts with echinoderms (Echi), benthic foraminifera (Bf) and ostracods (Ost) from bed RH 10. **f** Wackestone–packstone of bioclasts with fragments of bivalves (Biv), gastropods (Gast) and echinoderms (Echi) from bed RH 14. **g**, **h** Serpulids in a peloidal microbialite from bed RH 14

bers. Gastropods and serpulids are locally very common in the top of this stratigraphic interval (Fig. 3g, h).

- Stratigraphic interval III (RH 14′ to RH 19, 5.4 m): alternation of white limestones and marls with lumpy interlayers rich in echinoids (mainly *Mecaster pseudofournelli* and *Hemiaster syriacus*, and minority *Hirudocidaris uniformis*), ammonites (*Vascoceras gamai* and *Vascoceras* sp.) and gastropods. The top of RH 14′ presents a very high abundance of *M. pseudofournelli*. In the microfacies, the gastropods and serpulids are locally very common, together with encrusting foraminifera (*Placopsilina*) and dark microbial crusts (beds RH 14′ and 15, Fig. 4a). The calcareous beds are usually bioturbated (small *Thalassinoides* and *Planolites*, Fig. 2d) and correspond to bioclastic wackestones to packstones with foraminifera (20–30% of bioclasts), mollusc fragments (15–30%) and echinoderm fragments (*Diadema* type, 5–10%) (Fig. 2a, b). The gastropods are very common in RH 17′ (*Tylostoma*, Fig. 2e). Planktic foraminifera with biserial arrangement of chambers are very common (heterohelicids; > 55%, mainly *Planoheterohelix reussi*, Fig. 5).
- Stratigraphic interval IV (RH 20 to RH 22, 0.7 m): It is composed by three calcareous beds with chert nodules. They are bioclastic packstones of foraminifera (30–60% of bioclasts), ostracods (3–5%), bivalve fragments (5–15%) and echinoderm plates (5%, mainly echinoids and ophiuroids; Fig. 2c, d).
- Stratigraphic interval V (RH 22′ to RH 29, 11.8 m): alternation of decimetric marls and limestone beds. The upper part of the marls presents a lumpy appearance and abundance of poorly-preserved fossil macroinvertebrates (echinoids, ammonites and gastropods). The calcareous beds are packstones rich in peloids and bioclasts (mainly small benthic foraminifera, 40–50%; ostracods, 10–15%, fragments of bivalves, 10–15%; echinoderms, 2–5%; and algae). This stratigraphic interval is also characterized by a record of thin-shelled bivalves (filaments s. Robaszynski et al. 1993b) oriented parallel to bedding with increasing values toward the top (5–10%) (Fig. 4c, d). Locally (bed RH 25′), heterohelicids and serpulids are very common (Fig. 4e). Trace fossils are frequent in the upper part of this stratigraphic interval.

- Stratigraphic interval VI (RH 29′ to RH 36, 14.4 m): Alternating marls and limestones with a thickening upward trend finishing with massive banks of limestones containing bioclasts and densely bioturbated (Fig. 2a, b). The base of the RH 29′ is characterized by high amount of the gastropod *Tylostoma* (Fig. 2e). They are wackstones to packstones with benthic foraminifera (5–40%), ostracods (2–10%), mollusc fragments (5–30%), echinoderm fragments (2–10%) and scarce filaments. The trace fossils, corresponding to *Thalassinoides*, increase toward the top of this stratigraphic interval (Fig. 2f). These *Thalassinoides* have a yellow infilling and they are from 16 to 25 mm in diameter. The carbonate banks at the top appear to maintain the thickness, creating a continuous cliff which spans ~ 15 km in the northwest face of the Djebel Rhoundjaïa.

4.2 Microfossil assemblages

The biostratigraphy of the Cenomanian–Turonian transition in the Eastern Saharan Atlas is poorly studied. Bassoullet and Damotte (1969), report foraminifera and ostracods of limited biostratigraphic interest. For biostratigraphic assignments, we follow the planktic foraminiferal biozones proposed by Robaszynski and Caron (1995) for the Cretaceous of the Tethys. According to the definition of the Global Stratotype Section and Point (GSSP) for the base of the Turonian stage (Kennedy et al. 2005), the C/T boundary is near the top of the *W. archaeocretacea* Biozone. Analysis of foraminifera and ostracods from the upper part of the section (RH 14–RH 36) from sieved samples reveals relevant biostratigraphic microfauna for correlation at regional and global scales (Fig. 5).

4.2.1 Foraminifera

4.2.1.1 Planktic foraminiferal distribution From the lower part of the section (RH 1–RH 14), only thin sections were analysed (no marly layers are present), showing a record of both unkeeled trochospiral forms with globular chambers (hedbergellids, mainly *M. delrioensis* and less common *Muricohedbergella planispira*) and strongly keeled trochospiral forms (planoconvex shape) with high chambers (*H. praehelvetica* and *Dicarinella* sp.) (Fig. 6). Very scarce trochospiral keeled forms correspond to *Rotalipora* spp. (Fig. 6j, k). The last occurrence of *Rotalipora* would indicate the potential top of the *Rotalipora cushmani* Zone at the top of bed RH 6 (Fig. 5). The beginning of the *W. archaeocretacea* Zone is signalled in the studied section by the absence of *R. cushmani* and the record of *H. praehelvetica* in bed RH 6. From RH 10 to RH 14 planktic foraminifera are absent (Fig. 5). According to the Robaszynski and Caron (1995) the base of the *W. archaeocretacea* Zone is defined
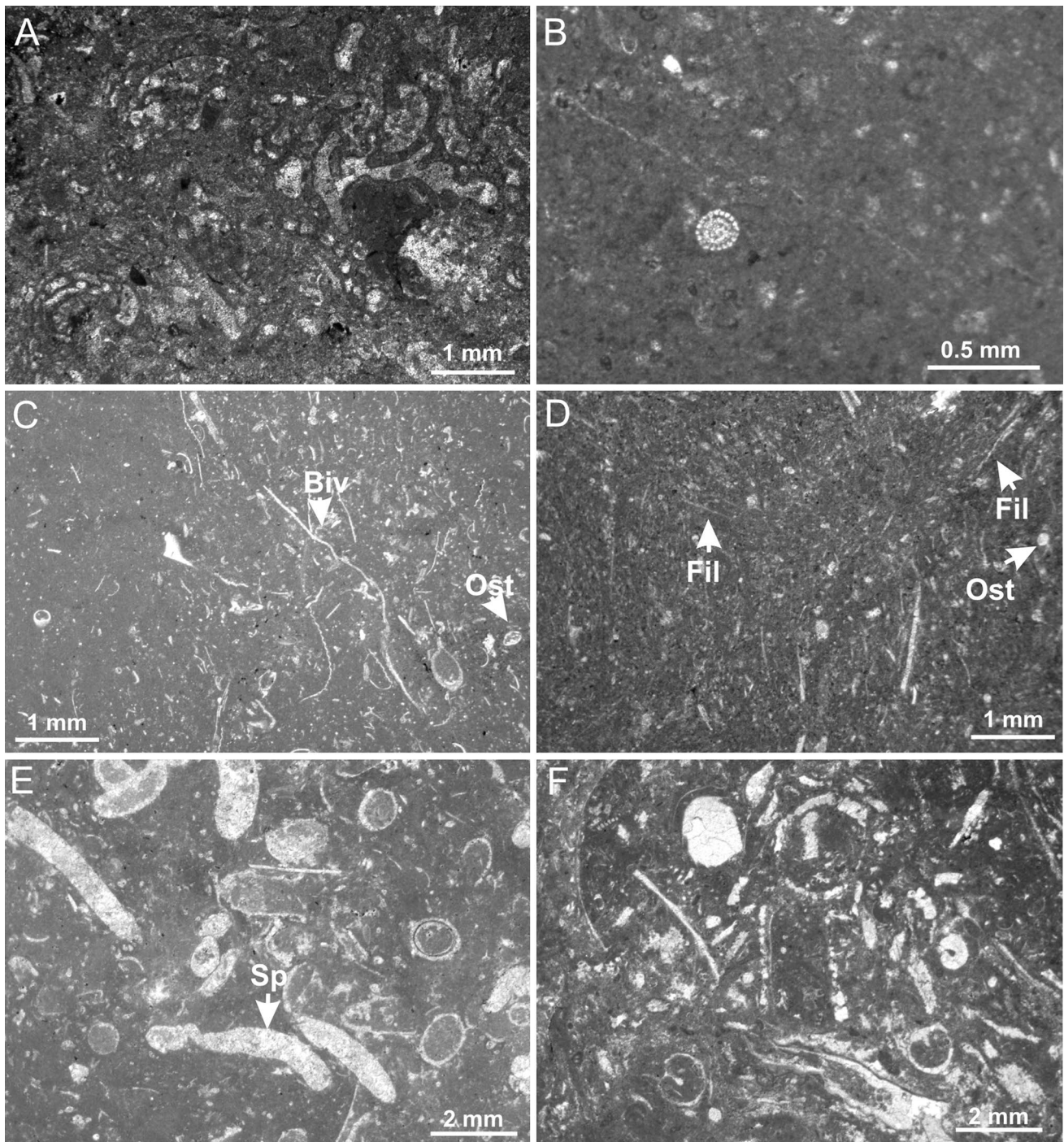
Fig. 4 Microfacies. **a** Detail of encrusting foraminifera from bed RH 14. **b** Wackestone with echinoderms and benthic foraminifera from bed RH 17. **c** Wackestone–packstone of bioclasts, mainly thin shelled bivalves (Biv) also called filaments and some ostracods (Ost) from bed RH 23. **d** Wackestone rich in filaments (Fil) from bed RH 24. **e** Packstone with abundant serpulids (Sp) from bed RH 25. **f** Packstone of bioclasts rich in fragments of gastropods and bivalves from bed RH 26

by the last occurrence of *R. cushmani* and the top is marked by the first occurrence of *Helvetoglobotruncana helvetica*.

At the top of RH 14, the unkeeled trochospiral forms with globular chambers are again registered. Planktic foraminifera showing a biserial arrangement of chambers are very common from sample RH 16 corresponding to heterohelicids. Analyses of the planktic foraminifera from sieved samples (RH 17′–RH 24′) pertaining to the upper

part of the Rhoundjaïa section point to a lowly diversified assemblage with only six species recorded. They correspond to biserial forms (*Planoheterohelix*), triserial forms (*Guembelitria*) and unkeeled trochospiral forms (*Muricohedbergella*). The recorded species are *Guembelitria cenomana* (Fig. 7a), *Guembelitria cretacea*, *M. planispira*, *M. delrioensis* (Fig. 7b), *Planoheterohelix moremani* (Fig. 7c, d) and *P. reussi* (Fig. 7e). The record of these taxa is not indicative of the Cenomanian–Turonian boundary; rather, they range from the *R. cushmani* Biozone (Upper Cenomanian) to *H. helvetica* Biozone (Lower Turonian) as reported in the Oued Bahloul section, a section of reference for studies of the North African palaeomargin (e.g. Reolid et al. 2015). *Planoheterohelix* reaches over 90% of the planktic foraminiferal assemblage from RH 17 to RH 24′. In the uppermost stratigraphic interval of Rhoundjaïa section (RH 25 to RH 36), planktic foraminifera are almost absent. Such a bloom of the heterohelicids has been reported in the lower half of the *W. archaeocretacea* Zone in other sections, including the Oued Bahloul section from the Central Tunisian Basin (Reolid et al. 2015), the Eastbourne section from South England (Keller et al. 2001) and Pueblo section from the Western Interior Basin (Leckie et al. 1998; Caron et al. 2006).

4.2.1.2 Benthic foraminiferal distribution The benthic foraminifera are numerous and diversified, yet they are not relevant for biostratigraphic purposes (Fig. 5). They are dominated by the agglutinated forms of the Family Lituolidae. Forms with calcitic shell are represented mainly by the Family Bolivinidae, characteristic of the Lower Turonian. Four main foraminiferal assemblages could be differentiated:

- The first benthic foraminiferal assemblage is recorded in the lowermost part of the section and is dominated by miliolids (*Quinqueloculina* sp.), and secondarily by textulariids (Figs. 3a, b, 6a–d).
- The second benthic foraminiferal assemblage is dominated by *Ammobaculites*. A total of 12 taxa were identified: *Ammobaculites benuensis*, *Ammobaculites coprolithiformis* (Fig. 7f, g), *Ammobaculites turonicus*, *Ammobaculites* sp., *Ammobaculites impescus* (Fig. 7h), *Ammobaculites subcretacea* (Fig. 7i, j), *Ammotium* cf. *nwalium*, *Ammotium* sp., *Lingulogavelinella* sp., *Gavelinopsis* sp., *Bolivina* sp., and *Haplophragmoides* cf. *saheliense*. This assemblage is recorded in the lower part of the section (from bed RH 17 to RH 23, Upper Cenomanian).
- The third benthic foraminiferal assemblage presents a total of seven recognized taxa: *Ammobaculites* sp., *A. impescus*, *Bolivina incrassata* (Fig. 7k), *Bolivina plaita* (Fig. 7l), *Bolivina* sp. (Fig. 7m), *H.* cf. *saheliense*, and *Placopsilina* sp. The assemblage is recorded from bed

RH 24 to RH 28 and coincides with the bloom of the heterohelicids.

- The fourth benthic foraminiferal assemblage (from bed RH 29′ to RH 31) is characterized by the first record of *Gabonita levis* (Fig. 7n, o). This assemblage presents a total of 12 species: *A. impescus*, *A. subcretacea*, *Ammobaculites bauchensis*, *Ammobaculites stephensonis* (Fig. 7p), *Ammobaculites fragmentarius* (Fig. 7q), *B. incrassata*, *B. plaita*, *G. levis*, *Gavelinella* sp. (Fig. 7r), *H.* cf. *saheliense*, *Haplophragmoides* sp., and *Tritascilina* sp. The record of *G. levis* indicates Lower Turonian. Together with this assemblage, some specimens of planktic foraminifera have been recorded (mainly *P. moremani* and *P. reussi*).
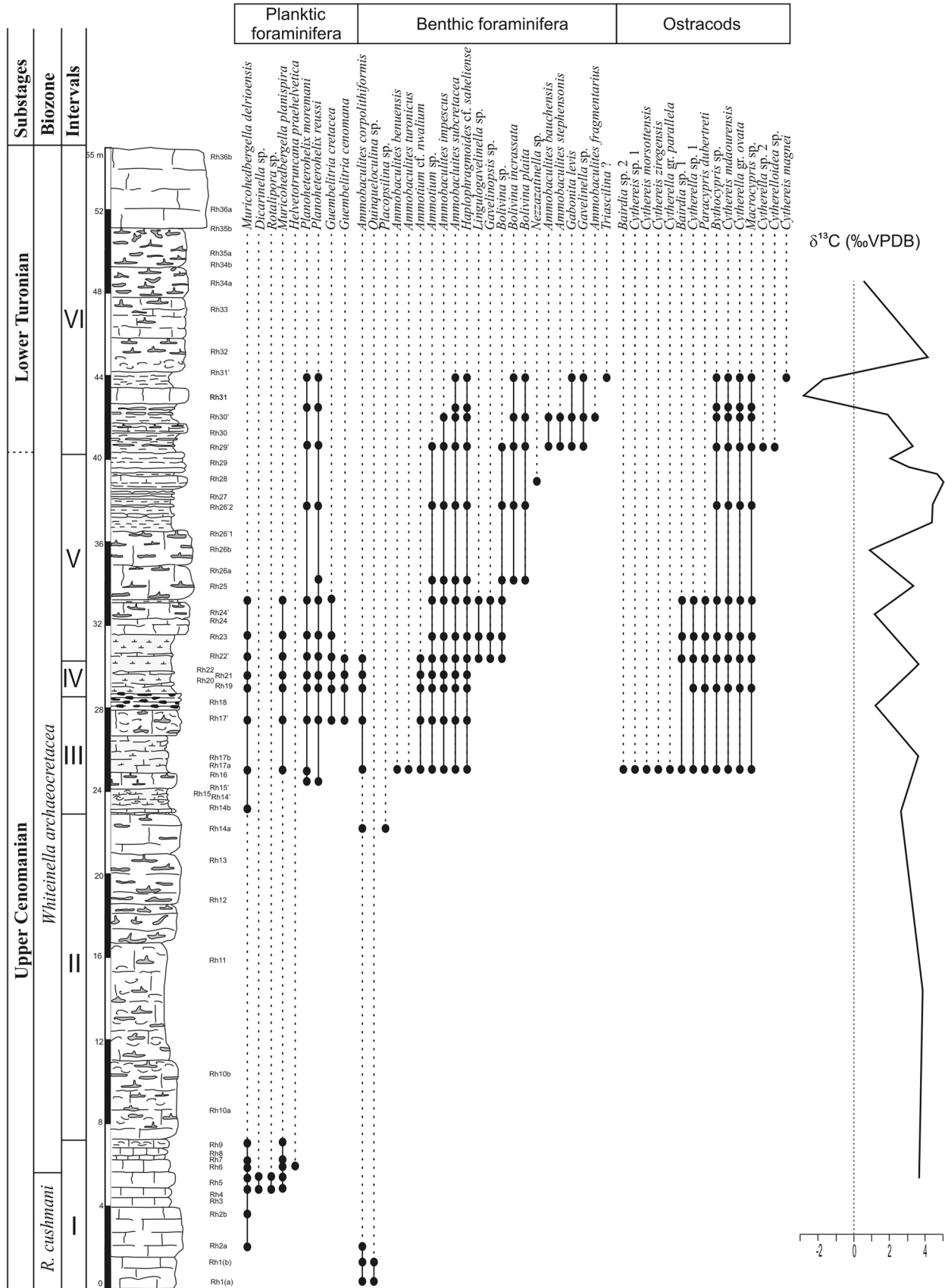
4.2.2 Ostracods

The ostracods of the Cenomanian–Turonian transition of the Eastern Saharan Atlas have been described and figured only by Bassoullet and Damotte (1969), and they remain in consideration as endemic species. From the biostratigraphic point of view, two ostracod assemblages can be identified in the upper part of the Rhoundjaïa section from sieved samples.

- The first assemblage is very diverse, made up of 13 species: *Cytherella* gr. *ovata* (Fig. 8a–c), *Cytherella* gr. *parallela*, *Cytherella* sp.1 (Fig. 8d, e), *Paracypris dubertreti* (Fig. 8f), *Paracypris mdaourensis* (Fig. 8g, h), *Bythocypris* sp. (Fig. 8i), *Macrocypris* sp. (Fig. 8j), *Bairdia* sp.1 (Fig. 8k), *Bairdia* sp.2 (Fig. 8l), *Cythereis ziregensis*, *Cythereis morsottensis*, *Cythereis mdaourensis* (Fig. 8m–o), and *Cythereis* sp. 1. This assemblage indicates the Upper Cenomanian. In Northern Africa the assemblage has been identified in the Eastern Saharan Atlas as corresponding to the *Cythereis algeriana* Zone, defined in Tunisia (Bismuth et al. 1981) and Egypt (Ismail 2001), or the *Cythereis* sp. assemblage Zone cited by Shahin (1991) in Egypt.
- The second ostracod assemblage is less diverse, featuring only seven species: *Bythocypris* sp., *Cytherella* sp. 2 (Fig. 8p), *C. mdaourensis*, *Cythereis magnei* (Fig. 8q), *Cytherelloidea* sp. (Fig. 8r), *Macrocypris* sp. and *P. mdaourensis*. This assemblage is recorded from sampling level RH 29 and corresponds to the *C. mdaourensis* Zone (Bismuth et al. 1981) which is located in the base of the Lower Turonian.

4.3 Bioevents

The Cenomanian–Turonian transition in the Rhoundjaïa Formation is marked by biologic events related to palaeoenvironmental and palaeoceanographic changes at the local

◀**Fig. 5** The Rhoundajia section and the planktic foraminiferal biozones with the stratigraphic distribution of planktic and benthic foraminifera, ostracods and the $\delta^{13}C$ curve from bulk carbonate

and global scale. The stratigraphic position of each event is discussed here, in the overall context of other regions.

4.3.1 The Planoheterohelix shift

Atop the Upper Cenomanian, a first biologic event is recorded by a peak of abundance of heterohelicids, mainly *P. moremani*. This event entails biostratigraphic value, corresponding to the so-called "*Heterohelix* shift Zone" of Leckie (1985). Still, we prefer to call it the *Planoheterohelix* shift after Haynes et al. (2015). This significant event has been identified worldwide: in eastern Algeria (Ruault-Djerrab et al. 2012, 2014), Morocco (Ettachfini and Andreu 2005; Ettachfini et al. 2005; Lézin et al. 2012), in Tunisia (Robaszynski et al. 1990, 2010; Nederbragt and Fiorentino 1999; Caron et al. 1999, 2006; Soua 2011, 2013; Zagrarni et al. 2008; Zaghbib-Turki and Soua 2013; Reolid et al. 2015), in France (Takashima et al. 2009), in Switzerland (Westermann et al. 2010), in Spain (Nederbragt et al. 1998), in England (Keller et al. 2001), in North America (Leckie et al. 1998; Keller and Pardo 2004a), in Venezuela (Nederbragt et al. 1998) and in Mexico (Aguilera-Franco and Allison 2004). In the Rhoundjaïa Formation of the Ksour Mountains, a proliferation of small biserial globular forms (*P. moremani* and *P. reussi*) is recorded in beds RH 16 to RH 24′), reaching 91–98% of the planktic foraminifera. This bloom of heterohelicids in the Ksour Basin is not related to local palaeoecological conditions, but is instead related to global environmental changes affecting the Tethyan and Pacific domains.

4.3.2 The cytherellid event

This biotic event corresponds to a bloom of ostracods (from bed RH 24′ to RH 29′, Lower Turonian), mainly smooth forms represented by the species *C*. gr. *ovata*. These specimens are also characterized by small size (ranging from 470 to 400 μm). At a local scale this event coincides with the appearance of filaments and the disappearance of planktic foraminifera. A similar increase in cytherellids has been reported in Spain (Barroso-Barcenilla et al. 2011) and Egypt (Shahin and Elbaz 2013). After the sample RH 29′ the composition of the ostracod assemblage change and *C*. gr. *ovata* disappear.

4.3.3 Filament event

The term "filaments" designates juvenile forms of thin-shelled bivalves (e.g. Robaszynski et al. 1993b; Caron

et al. 2006). These small bivalves, which proliferate in nutrient-rich waters, have mass mortality when they reach anoxic waters (e.g. Jefferies and Milton 1965). In the North African palaeomargin a filament event has been associated with organic-rich facies in the Bahloul Formation of Tunisia (Maamouri et al. 1994; Nederbragt and Fiorentino 1999; Amédro et al. 2005; Caron et al. 2006; Robaszynski et al. 1994, 2010; Zagrarni et al. 2008; Soua 2011; Negra et al. 2011; Zaghbib-Turki and Soua 2013), in northeastern Algeria (Bahloul Formation; Naili et al. 1995; Ruault-Djerrab et al. 2012) and Morocco (Ben Cherrou Formation; Ettachfini et al. 2005). This event was also reported in the reference section at Pueblo (Colorado, USA; Caron et al. 2006) and the Eagle Ford Group (Texas, USA; Denne et al. 2014).

In the Ksour Basin, in the interval from beds RH 24 to RH 29 of the Rhoundjaïa Formation, filaments are recorded for the first time, after the "*Planoheterohelix* shift" event. These filaments are observed in the wackestones-packstones related to bivalve bioclasts and benthic foraminifera. Filaments are progressively more abundant upwards just to the proposed Cenomanian–Turonian boundary (bed RH 29′). This record makes it possible to confirm the spatial repartition of the filament event at the scale of the Atlas, from eastern Tunisia to western Morocco (Negra et al. 2011). However, the abundance of filaments in the studied section is lower than in the Bahloul Formation.

4.4 Carbon isotopic values

In the Rhoundjaïa section the $\delta^{13}C$ data range from -2.83 to 5.03‰ (Fig. 5). The isotopic curve shows an average value of 2.89‰ in the lower part of the section and a successively increasing trend from bed RH 26′ (4.37‰) that reaches maximum values in bed RH 27 (5.03‰). A subsequent decrease of values is recorded from beds RH 26″ to RH 31, showing a negative isotopic excursion (reaching -2.83‰). In the Cenomanian–Turonian transition, the $\delta^{13}C$ show high values coinciding with the filament and cytherellids bioevents.

Previous $\delta^{13}C$ data have been published for the Eastern Saharan Atlas (Ouled Naïl and Aurès Mountains; Chikhi-Aouimeur et al. 2010) and the Saharan Platform (Grosheny et al. 2013).

5 Interpretation

5.1 Correlations and discussion

The bioevents, as well as the isotopic curves, are compared below with other basins for the *W. archaeocretacea* Zone.
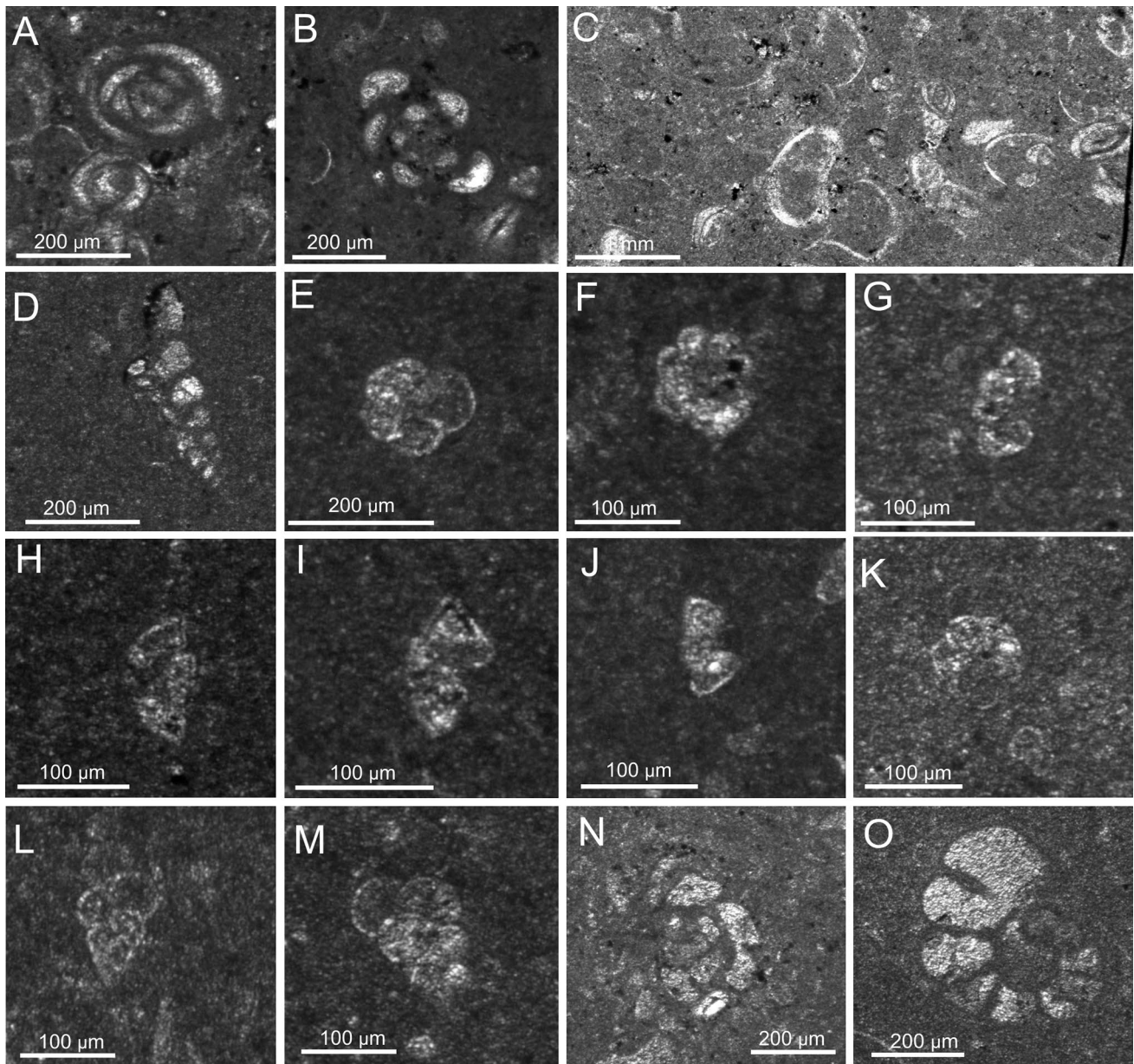
Fig. 6 Foraminifera from thin sections. **a**, **b** Miliolids from bed RH 1. **c** Ostracods and miliolids from RH 2. **d** Textularidae from RH 5. **e** *Muricohedbergella delrioensis* from RH 2. **f** *Muricohedbergella planispira* from RH 5. **g** *Helvetoglobotruncana praehelvetica* from RH 5. **h** Section with shape close to *Praeglobotruncana* and *Dicarinella* from RH 5. **i** Peripheric section of planktic foraminifera with characteristic features of *Rotalipora* (probably *brotzeni*) from bed RH 5. **j** *Rotalipora* from RH 5. **k** Umbilical section of *Muricohedbergella planispira* from bed RH 6. **l**, **m** *Planoheterohelix reussi* from bed RH 16. **n** Agglutinated foraminifera from RH 17. **o** *Nezzazatinella* (?) from RH 28

5.1.1 Comparison of planktic foraminiferal assemblages

The taxonomic composition of the planktic foraminiferal assemblages were compared with previous data from other North African and European basins using the software BG-Index 1.1 β (Escarguel 2001). The Simpson Index indicates the degree of relationship. The nine basins compared with the Ksour Basin are: Agadir Basin of Morocco (Jati et al. 2010), Central High Atlas of Morocco (Ettachfini et al. 2005), Tébessa Basin of Algeria (Ruault-Djerrab et al. 2012), Central Tunisia Basin (Soua 2011), Gabal Nezzazat, Egypt (Shahin 2007), NE Sicily, Italy (Scopelliti et al. 2004, 2008), Vocontian Basin, SE France (Tronchetti and Grosheny 1991), Iberian Basin (Barroso-Barcenilla et al. 2011), and Eastbourne Basin, S England (Keller et al. 2001). In this analysis the uncertain taxonomic categories

have been deleted (cf., gr. and aff.); it is finally constituted by a list of 38 species of planktic foraminifera, represented in a binary matrix of presence/absence (code 1: certified presence; code 0: probable absence). Based on the similarity matrix and the distances obtained by means of the Simpson Index, the connection between different basins could be derived using a Neighbour-Joining treatment. Three main groups were thereby identified (Figs. 9, 10):

- A first group contains three basins, Vocontian Basin (VB), Eastbourne Basin (EB) and Iberian Basin (IB). A total of 11 planktic species are shared between these three basins (28% of species): *Dicarinella algeriana*, *D. hagni*, *D. imbricata*, *M. delrioensis*, *M. planispira*, *W. archaeocretacea*, *W. baltica*, *W. brittonensis*, *Praeglobotruncana aumalensis*, *P. gibba*, and *P. stephani*. This group of basins representing the South-Northwest European Platform constitutes the main area of diversity at the specific level of planktic foraminifera.
- A second group corresponds to basins located in the Atlas—the Tébessa Basin (TB), Agadir Basin (AB), and Central High Atlas (CHA)— and shows a very similar specific composition with seven species in common: *M. delrioensis*, *Planoheterohelix globulosa*, *W. archaeocretacea*, *W. baltica*, *W. paradubia*, *P. gibba*, and *P. stephani*.
- The third group includes the eastern basins, that is, Ksour Basin (KB), NE Sicily (NES), Central Tunisia Basin (CTB) and Gabal Nezzazat, Egypt (SWS). This group is isolated in the phenogram and the Class Diagram. The analysis suggests a connection between Central Tunisia Basin (CTB) and NE Sicily (NES) in view of the diversified and homogeneous specific composition they share (*D. hagni*, *G. cenomana*, *M. planispira*, *M. simplex*, *P. moremani*, *Pl. reussi*, *W. aprica*, *W. archaeocretacea*, *W. aumalensis*, *W. baltica*, *Globigerinelloides bentonensis*, *G. ultramicra*, and *P. stephani*). The other two basins, Ksour Basin (KB) and Gabal Nezzazat, Egypt (SWS), both located in the northern palaeomargin of Africa, are completely isolated. The composition of planktic foraminifera is < 10% of the total list of species included in the analysis. Only four species are shared (*G. cenomana*, *M. planispira*, *P. moremani*, and *Pl. reussi*), and keeled morphotypes are absent.

The taxonomic data included in the software BG-Index 1.1 β (Escarguel 2001) show a biogeographic gradient from groups I to III, passing through group II (Figs. 9, 10). Therefore, during the *W. archaeocretacea* Zone there is a binary similarity between the basins probably favoured by the connecting sea-ways and also similar environmental conditions (e.g. oxygenation degree, nutrients availability, trophic conditions, temperature or salinity). The microfaunal list analysed points to both Tethyan and Atlantic influences. The absence of keeled and globular forms from some basins is remarkable, most likely related to local environmental conditions. The planktic species recorded from basins such as the Ksour Basin (KB) and the Gabal Nezzazat Basin, Egypt (SWS) indicate similar environmental conditions as well as connections between both areas of the North African palaeomargin, may be related to distribution of currents (see also Scotese 2011) advancing along the palaeomargin from east-to-west with a clockwise sense (Poulsen et al. 2001; Hay 2009).

5.1.2 Comparison of δ¹³C

The Cenomanian–Turonian transition (*W. archaeocretacea* Zone) is recorded in other regions of the world by an important carbon isotopic excursion (Jenkyns 1980; Hilbrecht and Hoefs 1986; Jarvis et al. 1988; Peryt and Wyrwicka 1991; Accarie et al. 1996; Hilbrecht et al. 1996; Hasegawa 1997; Nederbragt and Fiorentino 1999; Amédro et al. 2005; Keller et al. 2001, 2004; Caron et al. 2006; Grosheny et al. 2008, 2013; Karakitsios et al. 2007; Shahin 2007; Soua and Tribovillard 2007; Luciani and Cobianchi 1999; Westermann et al. 2010; Yilmaz et al. 2010; Hardas et al. 2012; Aquit et al. 2013; Prokoph et al. 2013).

However, the maximum values of the positive carbon isotopic excursion are diachronous, located below the Cenomanian–Turonian boundary, probably related to the diachronous record of planktic foraminifera (see Desmares et al. 2007; Mort et al. 2007; Paul and Lamolda 2009). The position of the carbon isotopic excursion is variable with respect to the anoxic interval. The *W. archaeocretacea* Zone is characterized by relatively higher values than the *R. cushmani* Zone both in the North African Margin and South European Margin (Fig. 11). However, the maximum values in this positive trend are recorded in variable position within the *W. archaeocretacea* Zone. The upper part of the *W. archaeocretacea*, around to the Cenomanian–Turonian boundary is characterized by a negative carbon isotopic excursion as recorded in the Aït Lamine Fm (Agadir Basin, Morocco; Jati et al. 2010), Tarfaya (Morocco, Tsikos et al. 2004), Oued Bahloul Fm (Central Tunisian Atlas; Caron et al. 2006) and Rhoundjaïa Fm in the Ksour Basin (Algeria) as evidenced in this study. Low values of δ¹³C are recorded also in South European Margin, but they are not a peak (e.g. the Iberian Basin, Barroso-Barcenilla et al. 2011; the Vocontian Basin in France, Takashima et al. 2009; Umbria Marche in Italy, Tsikos et al. 2004). In central Europe, the peak of the CIE is more delayed with respect to the Cenomanian–Turonian boundary, as seen for the Plenus Marls and Ballard Cliff Member (Eastbourne; Keller et al. 2001).
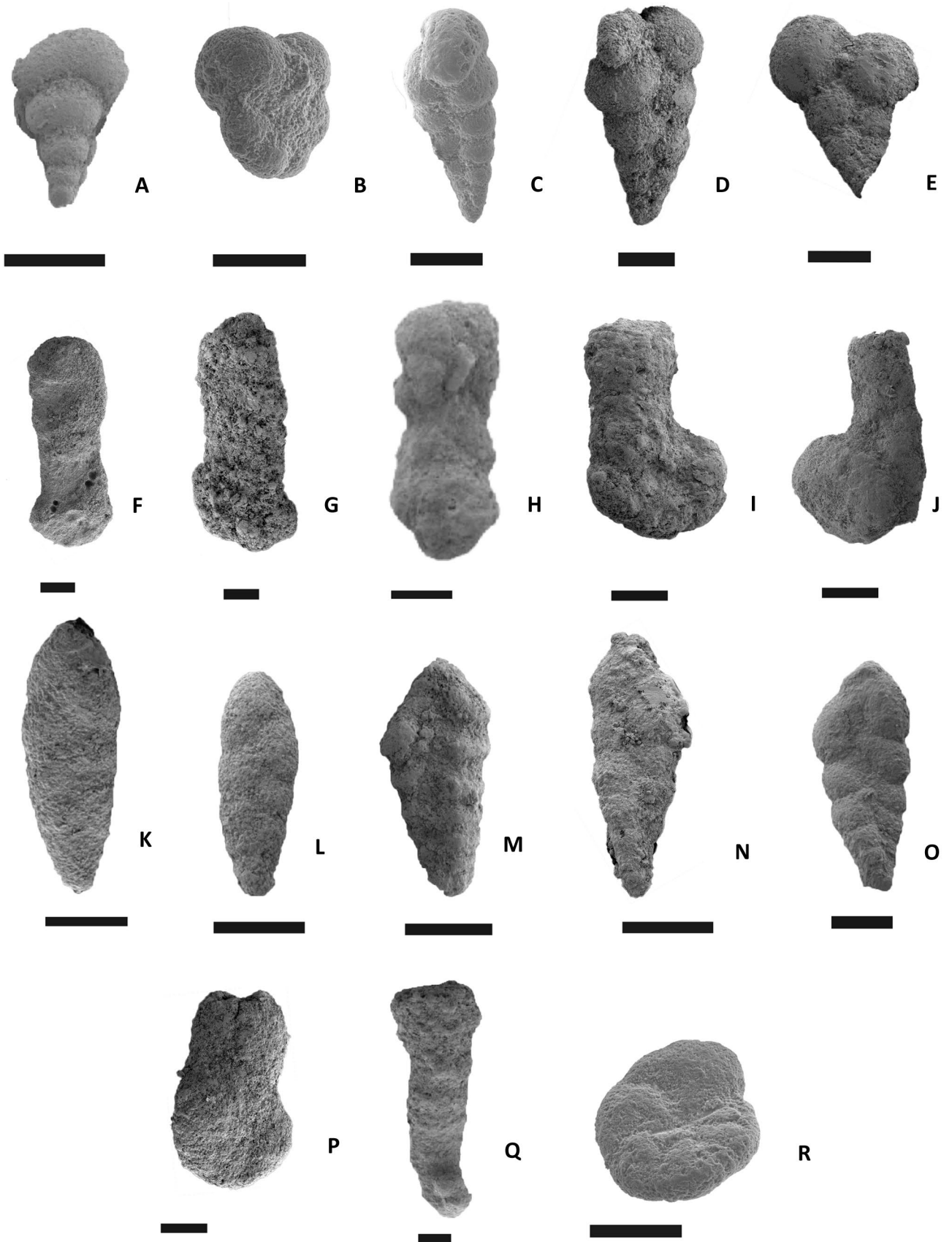
◂**Fig. 7** SEM illustrations of planktonic and benthic foraminifera from the Cenomanian and Turonian of the Rhoundjaia Formation. **a** *Guembelitria cenomana* (RH 17′). **b** *Muricohedbergella delrioensis* (RH 17′). **c**, **d** *Planoheterohelix moremani* (RH 17′). **e** *Planoheterohelix reussi* (RH 24′). **f**, **g** *Ammobaculites coprolithiformis* (RH 17′). **h** *Ammobaculites impescus* (RH 30′). **i**, **j** *Ammobaculites subcretacea* (RH 31′). **k** *Bolivina incrassata* (RH 29′). **l** *Bolivina plaita* (RH 29′). **m** *Bolivina* sp. (RH 29′). **n**, **o** *Gabonita levis* (RH 29′). **p** *Ammobaculites stephensonis* (RH 30′). **q** *Ammobaculites fragmentarius* (RH 31′). **r** *Gavelinella* sp. (RH 29′). Scalebar 100 µm

Therefore, the positive carbon isotopic excursion recorded in the Rhoundjaïa Formation (Ksour basin) shows a stratigraphic distribution that is similar to those of other Tethys basins, especially in the North African palaeomargin.

5.2 Palaeoenvironmental interpretation

Planktic and benthic foraminifera with assemblages consisting of low diversity and low oxygen tolerant species reflect a carbonate platform with nutrient-rich dysoxic conditions, but not anoxic conditions. Planktic foraminiferal assemblages are characterized by small simple morphologies (r-strategists, *Planoheterohelix* and *Guembelitria*) that mainly lived in the upper water column (Hart 1999; Price and Hart 2002; Keller and Pardo 2004b; Gertsch et al. 2008). Most isotopic data from Cenomanian–Turonian planktic foraminifera are consistent with a shallow habitat for heterohelicids (e.g. Corfield et al. 1990; Price et al. 1998; Price and Hart 2002). Deep-dwellers opportunist *Muricohedbergella*, mainly *M. delrioensis*, has been reported from oxygen depleted environments (Coxall et al. 2007; Ando et al. 2010; Reolid et al. 2016). Hedbergellids were traditionally considered shallow-water taxa but isotopic analyses indicate they were adapted to a wide range of depth probably overlapping with rotaliporids (Norris and Wilson 1998; Price et al. 1998). Keeled forms were recorded only in the lower part of the section represented by *Rotalipora* sp. and *Dicarinella* sp., both intermediate to deep-dweller specialists (Keller et al. 2001; Coccioni and Luciani 2004; Keller and Pardo 2004a, b). The low oxygen tolerant heterohelicids and hedbergellids are the first to colonize new seaways and ecospaces and among the last to survive in shallow neritic environments (Keller and Pardo 2004a, b; Gertsch et al. 2008). These shallow environments are often characterized by high nutrients due to terrigenous input, and occasionally low salinity due to fresh water influx.

From the base of the Rhoundjaïa section, different palaeoenvironmental fluctuations can be recorded according to the microfacies and microfossil assemblages (Fig. 12).

The lower part of the section (RH 1 to RH 9) with dominant mudstones and wackestones rich in planktic foraminifera indicate a clear influence of offshore conditions. The record of keeled forms of planktic foraminifera (*Rotalipora*, *Helvetoglobotruncana* and *Dicarinella*) is indicative of stable oligotrophic to mesotrophic conditions as well as the presence of intermediate to surface-dweller specialists (see Reolid et al. 2016). This is congruent with the assemblages and the inferred environmental conditions of the Upper Cenomanian recorded in the Betic Cordillera (Reolid et al. 2016).

The next stratigraphic interval (RH 10 to RH 14) is characterized by a higher influence of benthic components in the microfacies (bivalves, echinoids, foraminifera, gastropods, ophiuroids, ostracods, serpulids and trace makers) and the decrease of planktic foraminifera. These trends suggest a relative drop in sea-level and a shift from open marine to a middle neritic palaeoenvironment. However, sedimentary structures indicating high energy conditions are not recorded and indicate a depth below storm wave base. The bloom of small gastropods and serpulids, together with the presence of sessile agglutinated foraminifera, at the top of this interval may be related to changes in the cohesion degree of the sea bottom and opportunist colonization. Planktic foraminifera are very scarce; they newly appear in the top (RH 14) as unkeeled trochospiral forms with globular chambers, a morphogroup probably corresponding to more opportunist forms, that indicate relatively mesotrophic conditions (see planktic foraminiferal morphogroups of Reolid et al. 2016).

The next stratigraphic interval shows successive blooms (RH 14′–RH 22) of different benthic organisms such as small echinoids *M. pseudofournelli* and gastropods. High contents of gastropods and echinoids have been reported in conjunction with biotic stress during an initial phase of the OAE2 in the Sinai (Egypt) by Gertsch et al. (2008) related with rising sea-level. Moreover, gastropods, serpulids, encrusting foraminifera *Placopsilina* and microbialite are locally very abundant (bed RH 15), indicating a higher degree of sea bottom cohesion, a potential decrease in sedimentation rate and the opportunist colonization of the sea bottom. This is congruent with a transgressive trend (Fig. 12). In addition, the pelagic influence is consistent with the record of ammonites and planktic foraminifera. The record of biserial planktic foraminifera (*Planoheterohelix*) would indicate eutrophic conditions and the transition from oxygenated to poorly oxygenated waters (Reolid et al. 2015, 2016). Heterohelicids may be interpreted as low oxygen tolerant, blooming in stratified open marine settings (e.g. Keller et al. 2001; Coccioni and Luciani 2004; Keller and Pardo 2004a; Reolid et al. 2016). However, this part of the section shows abundant benthic fauna, and suboxic or anoxic conditions are excluded in this sector. Still, the increase of heterohelicid tests in this setting could indicate changes in the water column in distal and more pelagic environments. The increase in heterohelicids (*Heterohelix* shift) correlates with the abrupt increases recorded in the lower part of the *W. archaeocretacea* Zone of the Oued Bahloul section of Central Tunisia just before the
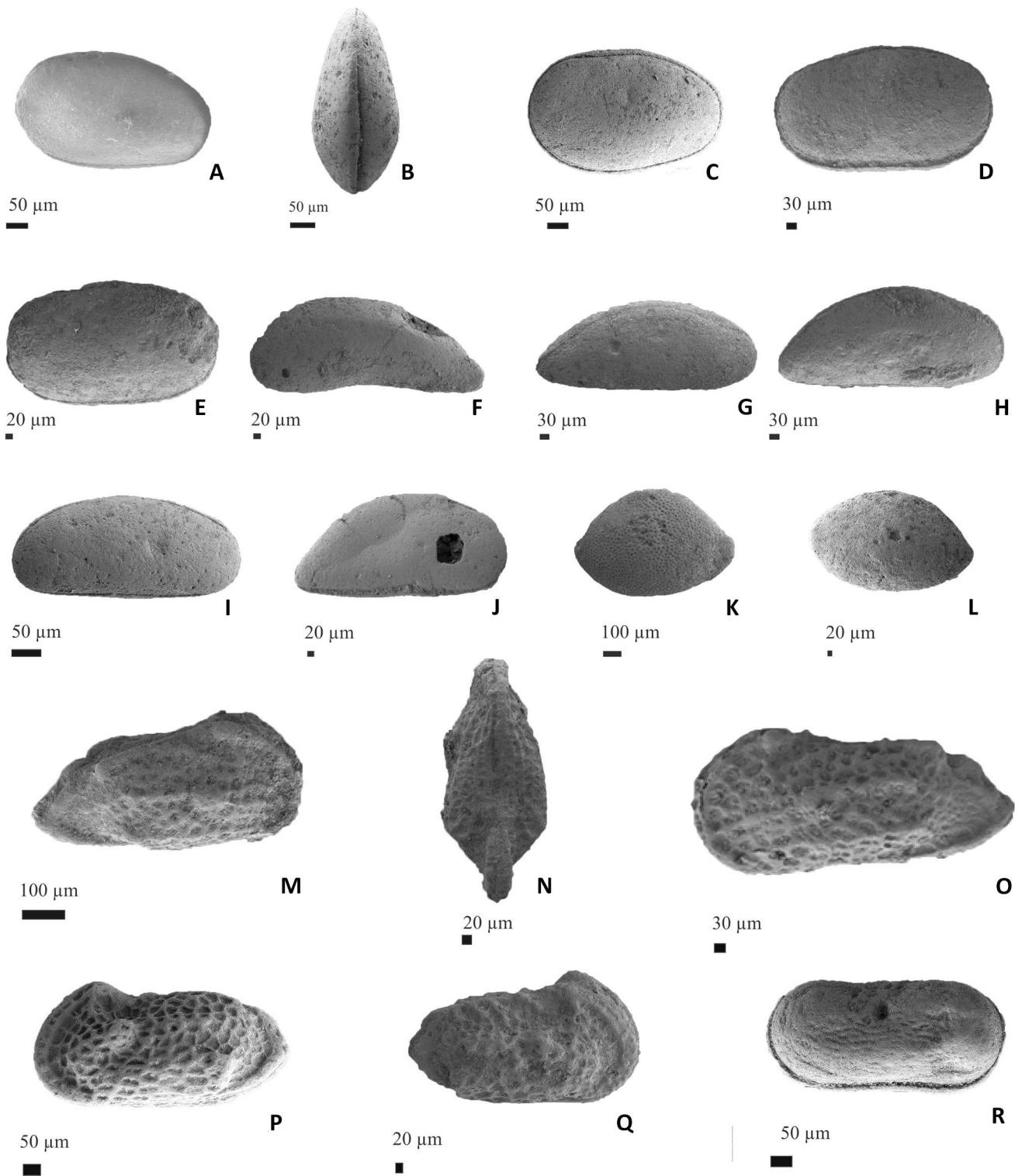
Fig. 8 SEM illustrations of ostracods from the Cenomanian and Turonian of the Rhoundjaia Formation. **a–c** *Cytherella* gr. *ovata* in right, dorsal and left views (RH 17′). **d, e** *Cytherella* sp.1. (RH 22′). **f** *Paracypris dubertreti* (RH 17′), **g, h** *Paracypris mdaourensis* (RH 29′). **i** *Bythocypris* sp. (RH 17′). **j** *Macrocypris* sp. (RH 17′). **k** *Bairdia* sp.1 (RH 17′). **l** *Bairdia* sp. 2 (RH 17′). **m–o** *Cythereis mdaouerensis* in lateral and dorsal views (RH 29′). **p** *Cythereis* sp. (RH 31′). **q** *Cythereis magnei* (RH 31′). **r** *Cytherelloidea* sp. (RH 17′)
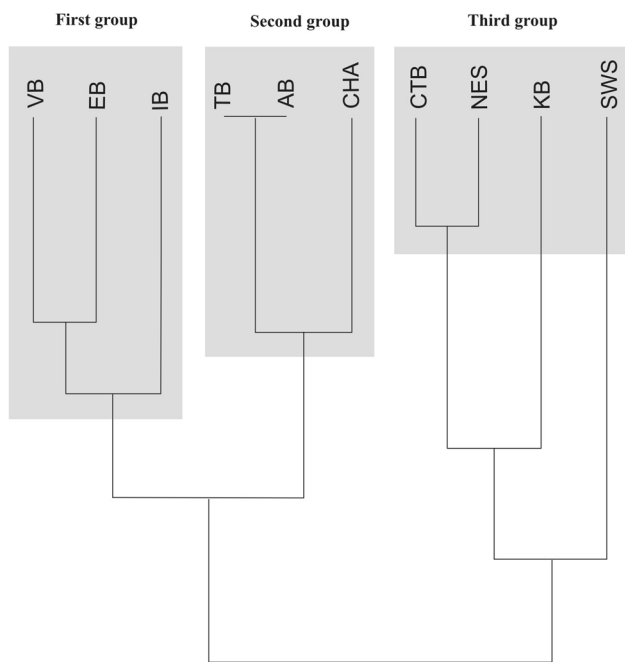
Fig. 9 Phenogram (tree of neighbour-joining) allowing the visualization of the proximity relationships between basins. *AB* Agadir Basin, *CHA* Central High Atlas, *CTB* Central Tunisia Basin, *EB* Eastbourne Basin, *IB* Iberian Basin, *KB* Ksour Basin, *NES* North East Sicily, *SWS* Jabal Nezzazat, *TB* Tébessa Basin, *Vb* Vocontian Basin
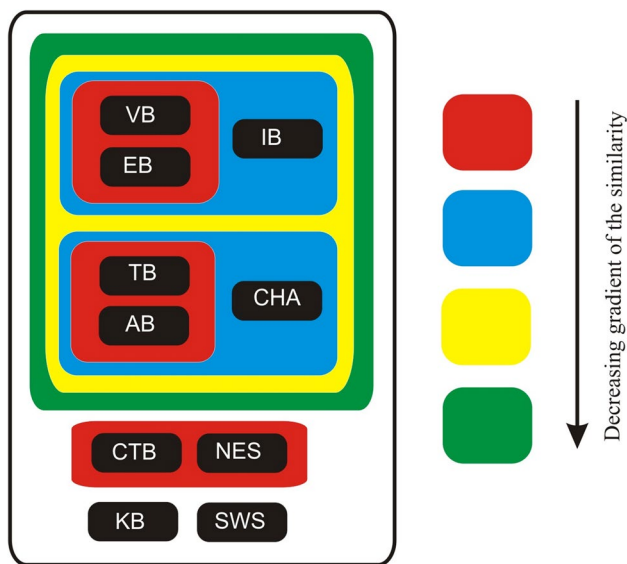

Fig. 10 Class diagram between basins. *AB* Agadir Basin, *CHA* Central High Atlas, *CTB* Central Tunisia Basin, *EB* Eastbourne Basin, *IB* Iberian Basin, *KB* Ksour Basin, *NES* North East Sicily, *SWS* Jabal Nezzazat, *TB* Tébessa Basin, *Vb* Vocontian Basin

OAE2 (Reolid et al. 2015). Yet depleted oxygen conditions are not recorded in this part of the palaeomargin. The low oxygen tolerant heterohelicids (surface-dweller opportunists) and hedbergellids (deep-dweller opportunists) colonized this relatively shallow neritic environment characterized by high nutrients due to terrigenous runoff and low salinity due to fresh water influx. In the Ksour Mountains these conditions are indicated not only by heterohelicids and hedbergellids, but also by the presence of textulariina (*Ammobaculites*) associated with hyaline species but without porcellaneous forms (e.g. Barnard et al. 1981; Wu et al. 2015).

The next stratigraphic interval (RH 22–RH 29) is characterized by a progressive diminution of heterohelicids (mainly from sampling bed RH 25′) and the increase of filaments and cytherellid ostracods. Heterohelicids survived whereas hedbergellids (deep-dwellers) disappeared. According to Leckie et al. (1991, 1998) biserial heterohelicids also tend to dominate marginal marine environments and they tolerated low salinity. Therefore, these trends may be related to a relative sea-level fall (or an advanced highstand). The record of well-preserved benthic macroinvertebrates such as bivalves, echinoids and gastropods, and nektonic organisms such as ammonites, confirm oxygenation at the sea bottom. The filament event, likewise reported in other parts of the Atlas from eastern Tunisia to western Morocco, has been interpreted as related to hemipelagic conditions during the maximum flooding (Zagrarni et al. 2008; Negra et al. 2011). However, the amount of filaments in the studied section are not comparable with examples from Tunisia and the context is not compatible with the maximum flooding.

The disappearance of planktic foraminifera in the Lower Turonian indicates particular palaeogeographic conditions of the Ksour Basin in comparison with the Tunisian Atlas and the Moroccan High Atlas where a maximum flooding and deepening (drowning phase) is recorded at the Cenomanian–Turonian boundary with black shales (Zagrarni et al. 2008; Negra et al. 2011; Reolid et al. 2015; Aguado et al. 2016). Only the record of ammonoids in the upper part of the section is congruent with the sea-level rise registered in the neighbouring regions.
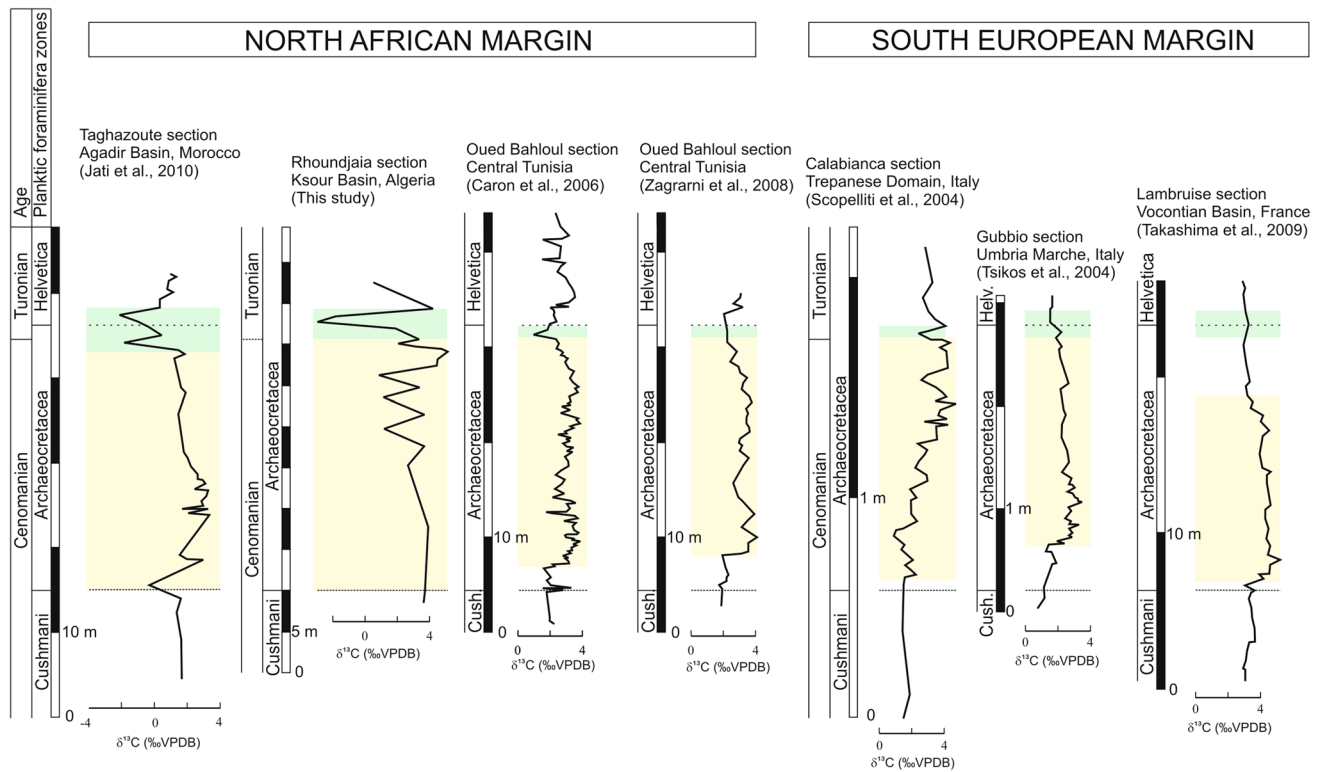
Fig. 11 Correlation of δ¹³C isotope curve of the Rhoundjaia Fm with some basins of the North African palaeomargin and basins of southern European palaeomargin

The uppermost part of the section (RH 29′–RH 36) shows a shallowing upward trend with an absence of planktic foraminifera and filaments, and an abundance of trace fossils. The low diversity of the benthic foraminiferal assemblage—composed mainly by *Gabonita* and *Gavelinella*—may be a relatively good indicator of shelf environments (Gebhardt et al. 2004). *G. levis* is known as an indicator of high flux of organic matter and related to oxygen depletion in the Latest Cenomanian and Early Turonian (Gebhardt et al. 2004). The extremely low diversity of *Gabonita* dominated assemblages is congruent with restricted conditions.

Therefore, this part of the Atlasic Basin, with shallow environments prone to major changes related to OAE2

related to nutrients availability and oxygenation throughout the Cenomanian–Turonian boundary but the incidence was lower than in neighbour areas of the Western Tethys. Typical open ocean sites such as Demerara Rise (Western South Atlantic, Oued Bahloul (Southwestern Tethys) and Subbetic (South Iberian Palaeomargin, Western Tethys) are affected by expanded OMZ in the water column.

Bottom water oxygenation in the Rhoundjäia section was controlled by a combination of water mass source and mixing and sea-level changes. The shallow environments of this area of the trans-Saharan seaway, flooded during sea-level rise of the Cenomanian–Turonian transition and poorly oxygenated deep waters reach the carbonate platform favouring the nutrification (upwelling) and proliferation of opportunists such as *Planoheterohelix* and *Muricohedbergella*. The proposed model has coincidences with the Guerrero-Morelos Platform (southern Mexico) where the Cenomanian shallow platform setting was affected by expansion of the OMZ during the sea-level rise of the Cenomanian/Turonian transition (Hernández-Romano et al. 1997). However, the magnitude of the drowning in Guerrero-Morelos Platform was higher than in the studied area of the Atlasic Basin and oxygen-poor waters and increasing depth exterminate the
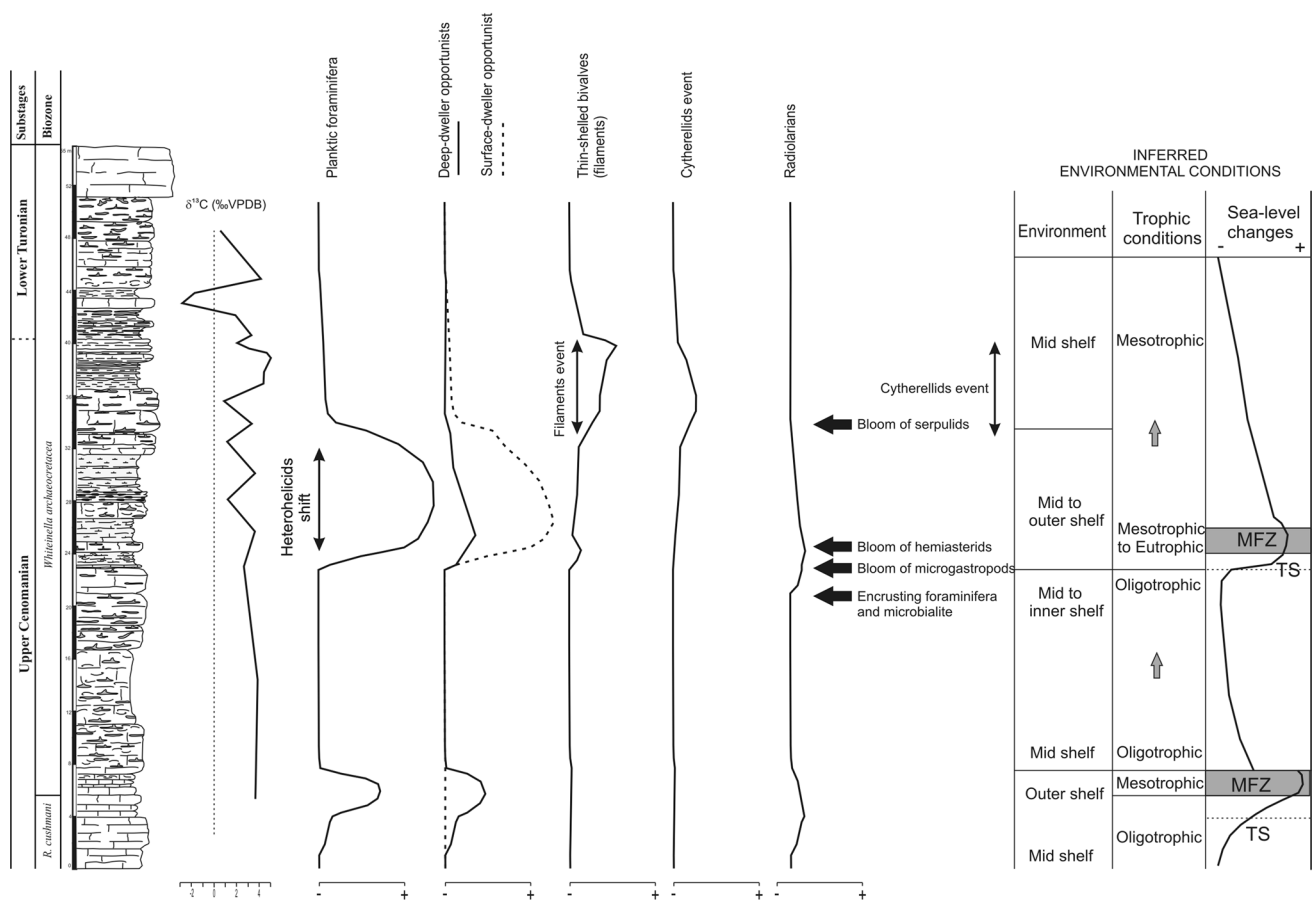
Fig. 12 Distribution of the δ¹³C values, distribution of planktic foraminifera, thin-shelled bivalves, radiolarians and main bioevents in the studied section and the inferred environmental conditions (environment within the shelf trophic conditions and sea-level trends)

benthic carbonate production. According to Hernández-Romano et al. (1997) subsidence had an important role in this area.

This pattern is clearly different to the model proposed by Elderbak et al. (2014) and Lowery et al. (2018) for the Western Interior Basin, where deoxygenation in shallow environments was controlled by estuarine-circulation in a semi-restricted basin.

6 Conclusions

During the Late Cenomanian–Early Turonian, the Ksour Basin constituted a mid to outer shelf environment where relative sea-level changes were recorded in the faunal assemblages by changes in the neritic/pelagic influence. Benthic and planktic foraminiferal assemblages, consisting of low diversity and low oxygen tolerant species, reflect a carbonate platform with biotic stress conditions. During *W. archaeocretacea* Zone, planktic foraminiferal assemblages

were dominated by opportunists such as *Muricohedbergella* (deep-dweller), *Planoheterohelix* and *Guembelitria* (surface-dwellers), which colonized new ecospace in the shelf when the sea-level rose (heterohelicid shift). The OAE2 is not reflected in the studied section by organic rich facies, yet its impact can be also identified through the successive proliferation of different organisms such as microgastropods and echinoid hemiasterids just before the heterohelicid shift. The continuous presence of trace fossils and benthic macroinvertebrates allows us to exclude oxygen depleted conditions. The proliferation of *Planoheterohelix* in the *W. archaeocretacea* Zone marks the record of eutrophic conditions and the transition from oxygenated to poorly oxygenated waters during stratified open marine settings that were favoured by marine flooding. The subsequent increase in thin-shelled bivalves and cytherellid ostracods confirm the stress conditions at the time of the δ¹³C isotopic excursion. The onset of the Turonian is accompanied by a shallowing upward trend in the Ksour Basin, while neighbouring regions such as the

Tunisian Atlas and Moroccan High Atlas record a maximum flooding and deepening with black shales.

Comparison of the taxonomic composition of the planktic foraminiferal assemblages (phenogram and class diagram) points to a closer relationship between the Ksour Basin and the Northeast Sicily Basin, Central Tunisia Basin and Egypt, as opposed to other basins in southern Europe and in Morocco. This context means potential geographic connection or similar environmental conditions. Notwithstanding, the comparison indicates that the Ksour Basin was relatively isolated with respect to surrounding basins.

References

Accarie, H., Emmanuel, L., Robaszynski, F., Baudin, F., Amédro, F., & Caron, M. (1996). La géochimie isotopique du carbone comme outil stratigraphique. Application a` la limite Cénomanien–Turonien en Tunisie Centrale. *Comptes Rendus de l'Académie des Sciences, Paris, 322,* 579–586.

Accarie, H., Robaszynski, F., Amédro, F., Caron, M., & Zagrarni, M. F. (2000). Stratigraphie événementielle au passage Cénomanien–Turonien dans le secteur occidental de la plate-forme de Tunisie centrale (Formation Bahloul, région de Kalaat Senan). *Annales des Mines et de la Géologie. Tunis, 40,* 63–80.

Aguado, R., Reolid, M., & Molina, E. (2016). Response of calcareous nannoplankton to the Late Cretaceous oceanic anoxic event 2 at Oued Bahloul (Central Tunisia). *Palaeogeography, Palaeoclimatology, Palaeoecology, 459,* 289–305.

Aguilera-Franco, N., & Allison, P. (2004). Events of the Cenomanian–Turonian Succession, Southern Mexico. *Journal of Iberian Geology, 31,* 25–50.

Aït Ouali, R., & Delfaud, J. (1995). Les modalités d'ouverture du bassin des Ksour au Lias dans le cadre du «rifting» jurassique au Maghreb. *Comptes Rendus de l'Académie des Sciences, Paris, 320,* 773–778.

Aly, M. F., & Abdel-Gawad, G. I. (2001). Upper Cenomanian–Lower Turonian ammonites from north and central Sinai, Egypt. *El-Minia Science Bulletin, 13,* 17–60.

Amédro, A., Accarie, H., & Robaszynski, F. (2005). Position de la limite Cénomanien–Turonien dans la Formation Bahloul de Tunisie centrale: Apports intégrés des ammonites et des isotopes du carbone (δ^{13}C). *Eclogae Geologicae Helvetiae, 98,* 151–167.

Ando, A., Huber, B. T., & MacLeod, K. G. (2010). Depth-habitat reorganization of planktonic foraminifera across the Albian/Cenomanian boundary. *Paleobiology, 36,* 357–373.

Andreu, B. (2002). Cretaceous ostracode biochronology of Morocco. *Eclogae Geologicae Helvetiae, 95,* 133–152.

Andreu, B., Lebedel, V., Wallez, M. J., Lézin, C., & Ettachfini, M. (2013). The upper Cenomanian lower Turonian carbonate platform of the Preafrican Trough, Morocco: Biostratigraphic, paleoecological and paleobiogeographical distribution of ostracods. *Cretaceous Research, 45,* 1–31.

Aquit, M., Kuhnt, W., Holbourn, A., Chellai, E. H., Stattegger, K., Kluth, O., et al. (2013). Late Cretaceous palleoenvironmental evolution of the Tarfaya Atlantic coastal Basin, SW Morocco. *Cretaceous Research, 45,* 288–305.

Arthur, M. A., & Schlanger, S. O. (1979). Cretaceous oceanic anoxic events as causal factors in development of reef-reservoired giant oil fields. *American Association of Petroleum Geologists Bulletin, 63,* 870–885.

Arthur, M. A., Schlanger, S. O., & Jenkyns, H. C. (1987). The Cenomanian–Turonian oceanic anoxic event, II. Palaeoceanographic controls on organic-matter production and preservation. *Journal of the Geological Society Special Publications, 26,* 401–420.

Ayoub-Hannaa, W., Huntley, J. W., & Fürsich, F. T. (2013). Significance of detrended correspondence analysis (DCA) in palaeoecology and biostratigraphy: A case study from the Upper Cretaceous of Egypt. *Journal of African Earth Sciences, 80,* 48–59.

Barnard, T., Cordey, W. G., & Shipp, D. J. (1981). Foraminifera from the Oxford Clay (Callovian–Oxfordian of England). *Revista Española Micropaleontología, 13,* 383–462.

Barroso-Barcenilla, F., Pascual, A., Peyrot, D., & Rodríguez-Lázaro, J. (2011). Integrated biostratigraphy and chemostratigraphy of the upper Cenomanian and lower Turonian succession in Puentedey, Iberian Trough, Spain. *Proceedings of the Geologists Association, 122,* 67–81.

Bassoullet, J. P., & Damotte, R. (1969). Quelques ostracodes nouveaux du Cénomanien–Turonien de l'Atlas saharien occidental (Algérie). *Revue de Micropaléontologie, 3,* 130–144.

Bauer, J., Kuss, J., & Steuber, T. (2002). Platform environments, microfacies and systems tracts of the Upper Cenomanian–Lower Santonian of Sinai. *Egypt. Facies, 47,* 1–25.

Benyoucef, M., Mebarki, K., Ferré, B., Adaci, M., Bulot, L. G., Desmares, D., et al. (2017). Litho- and biostratigraphy, facies patterns and depositional sequences of the Cenomanian–Turonian deposits in the Ksour Mountains (Saharan Altas, Algeria). *Cretaceous Research, 78,* 34–55.

Bismuth, H., Donze, P., Lefevre, J., & Saint-Marc, P. (1981). Nouvelles espèces d'ostracodes dans le Crétacé Moyen et Supérieur du Djebel Semmama (Tunisie du Centre-Nord). *Cahiers de Micropaléontologie, 3,* 51–69.

Bornemann, A., Norris, R. D., Friedrich, O., Beckmann, B., Schouten, R., Sinninghe-Damste, J., et al. (2008). Isotopic evidence for glaciation during the Cretaceous super-greenhouse. *Science, 319,* 951–954.

Busson, G., & Cornée, A. (1996). L'événement océanique anoxique du Cénomanien supérieur-terminal: une revue et une interprétation mettant en jeu une stratification des eaux marines par le CO_2 mantellique. *Sociéte Géologique du Nord, 23,* 143.

Busson, G., Dhondt, A., Amédro, F., Néraudeau, D., & Cornée, A. (1999). La grande transgression du Cénomanien supérieur–Turonien inférieur sur la Hamada de Tinrhert (Sahara algérien): Datations biostratigraphiques, environnements de dépôt et comparaison d'un témoin épicratonique avec les séries contemporaines à matière organique du Maghreb. *Cretaceous Research, 20,* 29–46.

Caron, M., Dall' Agnolo, S., Accarie, H., Barrera, E., Kauffman, E. G., Amédro, F., et al. (2006). High-resolution stratigraphy of the Cenomanian–Turonian boundary interval at Pueblo (USA) and wadi Bahloul (Tunisia): Stable isotope and bio-events correlation. *Geobios, 39,* 171–200.

Caron, M., Robaszynski, F., Amédro, F., Baudin, F., Deconinck, J. F., Hochuli, P., et al. (1999). Estimation de la durée de l'événement anoxique global au passage Cénomanien/Turonien. Approche cyclostratigraphique dans la formation Bahloul en Tunisie centrale. *Bulletin Société Géologique France, 170,* 145–160.

Chikhi-Aouimeur, F., Grosheny, D., Ferry, S., Harket, M., Jati, M., Atrops, F., et al. (2010). Lithofaciès, paléogéographie et corrélations au passage Cénomanien–Turonien dans l'Atlas Saharien (Ouled Naïl, Zibans, Aurès et Hodna, Algérie). *Mémoire du Service Géologique National d'Algérie, 17,* 67–83.

Coccioni, R., & Luciani, V. (2004). Planktonic foraminifera and environmental changes across the Bonarelli Event (OAE2, latest Cenomanian) in its type area: A high-resolution study from the Tethyan reference Bottaccione section (Gubbio, Central Italy). *Journal of Foraminiferal Research, 34,* 109–129.

Corfield, R. M., Hall, M., & Brasier, M. D. (1990). Stable isotope evidence for foraminifeal habitats during the development of the Cenomanian/Turonian oceanic anoxic event. *Geology, 18,* 175–178.

Courville, P. (2007). Échanges et colonisations fauniques (Ammonitina) entre Téthys et Atlantique sud au Crétacé supérieur: Voies atlantiques ou sahariennes? *Carnets de Géologie, 2,* 1–19.

Courville, P., Meister, C., Lang, J., Mathey, B., & Thierry, J. (1991). Les corrélations en Téthys occidentale et l'hypothèse de la liaison Téthys-Atlantique sud: Intérêts des faunes d'ammonites du Cénomanian supérieur–Turonien moyen basal du Niger et du nigeria (Afrique de l' Ouest). *Comptes-Rendus de l'Académie des Sciences de Paris, 313,* 1039–1042.

Courville, P., Thierry, J., & Lang, J. (1998). Ammonites faunal exchanges between South Tethysian platforms and South Atlantic during the uppermost Cenomanian–Lowermost middle Turonian in the Benue Trough (Nigeria). *Geobios, 32,* 187–214.

Coxall, H. K., Wilson, P. A., Pearson, P. N., & Sexton, P. F. (2007). Iterative evolution of digitate planktonic foraminifera. *Paleobiology, 33,* 495–516.

Delfaud, J. (1986). Organisation scalaire des événements sédimentaires majeurs autour de la Mésogée durant le Jurassique et le Crétacé. Conséquences pour les associations biologiques. *Bulletin des Centres de Recherches Exploration –Production, Elf-Aquitaine, 10,* 205–206.

Denne, R. A., Hinote, R. E., Breyer, J. A., Kosanke, T. H., Lees, J. A., Engelhardt-Moore, N., et al. (2014). The Cenomanian–Turonian Eagle Ford Group of South Texas: Insights on timing and paleoceanographic conditions from geochemistry and micropaleontologic analyses. *Palaeogeography, Palaeoclimatology, Palaeoecology, 413,* 2–28.

Desmares, D., Grosheny, D., Beaudoin, B., Gardin, S., & Gauthier-Lafaye, F. (2007). High resolution stratigraphic record constrained by volcanic ash beds at the Cenomanian–Turonian boundary in the Western Interior Basin, USA. *Cretaceous Research, 28,* 561–582.

Elderbak, K., Leckie, R. M., & Tibert, N. E. (2014). Paleoenvironmental and paleoceanographic changes across the Cenomanian–Turonian boundary event (oceanic anoxic event 2) as indicated by foraminiferal assemblages from the eastern margin of the Cretaceous Western Interior Sea. *Palaeogeography, Palaeoclimatology, Palaeoecology, 413,* 29–48.

El-Sabbagh, A., Tantawy, A. A., Keller, G., Khozyem, H., Spangenberg, J., Adatte, T., et al. (2011). Stratigraphy of the Cenomanian–Turonian oceanic anoxic event OAE2 in shallow shelf sequences of NE Egypt. *Cretaceous Research, 32,* 705–722.

Erbacher, J., & Thurow, J. (1997). Influence of oceanic anoxic events on the evolution of mid Cretaceous radiolaria in the North Atlantic and western Tethys. *Marine Micropaleontology, 30,* 139–158.

Escarguel, G. (2001). BG. Index version 1.1β. Programme et notice d'utilisation.

Ettachfini, M., & Andreu, B. (2005). Le Cénomanien et le Turonien de la Plate-forme Préafricaine du Maroc. *Cretaceous Research, 25,* 277–302.

Ettachfini, M., Souhel, A., Andreu, B., & Caron, M. (2005). La limite Cénomanien–Turonien dans le Haut Atlas central, Maroc. *Geobios, 38,* 57–68.

Ferré, B., Mebarki, K., Benyoucef, M., Villier, L., Bulot, L. G., Desmares, D., et al. (2017). Roveacrinids (Crinoidea, Roveacrinida) from the Cenomanian–Turonian of southwest Algeria (Saharan Atlas and Guir Basin). *Annales de Paléonologie, 103,* 185–196.

Friedrich, O., Erbacher, J., & Mutterlose, J. (2006). Paleoenvironmental changes across the Cenomanian/Turonian boundary event (oceanic anoxic event 2) as indicated by benthic foraminifera from the Demerara Rise (ODP Leg 207). *Revue de Micropaléontologie, 49,* 121–139.

Gebhardt, H., Friedrich, O., Schenk, B., Fox, L., Hart, M., & Wagreich, M. (2010). Paleo-ceanographic changes at the northern Tethyan margin during the Cenomanian–Turonian oceanic anoxic event (OAE-2). *Marine Micropaleontology, 77,* 25–45.

Gebhardt, H., Kuhnt, W., & Holbourn, A. (2004). Foraminiferal response to sea level change, organic flux and oxygen deficiency in the Cenomanian of the Tarfaya Basin, southern Morocco. *Marine Micropaleontology, 53,* 133–157.

Gertsch, B., Keller, G., Adatte, T., Berner, Z., Kassab, A. S., Tantawy, A. A., et al. (2008). Cenomanian–Turonian transition in a shallow water sequence of the Sinai, Egypt. *International Journal of Earth Sciences, 99,* 165–182.

Grosheny, D., Chikhi-Aouimeur, F., Ferry, S., Benkherouf-Kechid, F., Jati, M., Atrops, F., et al. (2008). The Upper Cenomanian–Turonian (Upper Cretaceous) of the Saharan Atlas (Algeria). *Bulletin de la Société Géolologique de France, 179,* 593–603.

Grosheny, D., Ferry, S., Jati, M., Ouaja, M., Bensalah, M., Atrops, F., et al. (2013). The Cenomanian–Turonian boundary on the Saharan Platform (Tunisia and Algeria). *Cretaceous Research, 42,* 66–84.

Hardas, P., & Mutterlose, J. (2007). Calcareous nannofossil assemblages of oceanic anoxic event 2 in the equatorial Atlantic: Evidence of a eutrophication event. *Marine Micropaleontology, 66,* 52–69.

Hardas, P., Mutterlose, J., Friedrich, O., & Erbacher, J. (2012). The Middle Cenomanian Event in the equatorial Atlantic: The calcareous nannofossil and benthic foraminiferal response. *Marine Micropaleontology, 96–97,* 66–74.

Harket, M., & Delfaud, J. (2000). Genèse des séquences sédimentaires du Crétacé supérieur des Aurès (Algérie). Rôle de l'eustatisme, de la tectonique, de la subsidence: une mise au point. *Comptes Rendus Académie des Sciences, 330,* 785–792.

Harries, P. J. (1993). Dynamics of survival following the Cenomanian–Turonian (Upper Cretaceous) mass extinction event. *Cretaceous Research, 14,* 563–583.

Harries, P. J., & Kauffman, E. G. (1990). Patterns of survival and recovery following the Cenomanian–Turonian (Late Cretaceous) mass extinction in the Western Interior Basin, United States. *Lecture Notes in Earth History, 30,* 277–298.

Harries, P. J., & Little, C. T. (1999). The early Toarcian (Early Jurassic) and the Cenomanian–Turonian (Late Cretaceous) mass extinctions: Similarities and contrasts. *Palaeogeography, Palaeoclimatology, Palaeoecology, 154,* 39–66.

Hart, M. B. (1999). The evolution and diversity of Cretaceous planktonic foraminiferida. *Geobios, 32,* 247–255.

Hasegawa, T. (1997). Cenomanian–Turonian carbon isotope events recorded in terrestrial organic matter from northern Japan. *Palaeogeography, Palaeoclimatology, Palaeoecology, 130,* 251–273.

Hay, W. W. (2009). Cretaceous oceanic red beds: Stratigraphy, composition, origins and paleoceanographic and paleoclimatic significance. *SEPM Special Publication, 91,* 243–271.

Haynes, S. J., Huber, B. T., & MacLeod, K. G. (2015). Evolution and phylogeny of mid-Cretaceous (Albian–Coniacian) Biserial planktic foraminifera. *Journal of Foraminiferal Research, 45,* 42–81.

Hernández-Romano, U., Aguilera-Franco, N., Martínez-Medrano, M., & Barceló-Duarte, J. (1997). Guerrero-Morelos Platform drowning at the Cenomanian–Turonian boundary, Huitziltepec area, Guerrero State, southern Mexico. *Cretaceous Research, 18,* 661–686.

Hetzel, A., März, C., Vogt, C., & Brümsack, H. J. (2011). Geochemical environment of Cenomanian–Turonian black shale deposition at Wunstorf (northern Germany). *Cretaceous Research, 32,* 480–494.

Hilbrecht, H., Frieg, C., Troger, K. A., Voigt, S., & Voigt, T. (1996). Shallow water facies during the Cenomanian–Turonian anoxic event: Bio-events, isotopes, and sea level in southern Germany. *Cretaceous Research, 17,* 229–253.

Hilbrecht, H., & Hoefs, J. (1986). Geochemical and palaeontological studies of the δ13C anomaly in boreal and north tethyan Cenomanian–Turonian sediments in Germany and adjacent areas. *Palaeogeography, Palaeoclimatology, Palaeoecology, 53,* 169–189.

Huber, B. T., Norris, R. D., & McLeod, K. G. (2002). Deep-sea paleotemperature record of extreme warmth during the Cretaceous. *Geology, 30,* 123–126.

Ismail, A. A. (2001). Correlation of Cenomanian–Turonian ostracods of Jebel Shabraweet with their counterpart in Egypt, Nort Africa and the Middle East. *Neues Jahrbuch für Geologie und Paläontologie Monatshefte, 9,* 513–533.

Ismail, A. A., Hussein-Kamel, Y. F., Boukhary, M., & Ghandour, A. A. (2009). Late Cenomanian–Early Turonian foraminifera from Eastern Desert, Egypt. *Micropaleontology, 55,* 396–412.

Jarvis, I., Carson, G. A., Cooper, M. K. E., Hart, M. B., Leary, P. N., Tocher, B. A., et al. (1988). Microfossil assemblages and the Cenomanian–Turonian (late Cretaceous) oceanic anoxic event. *Cretaceous Research, 9,* 3–103.

Jarvis, I., Lignum, J. S., Gröcke, D. R., Jenkyns, H. C., & Pearce, M. A. (2011). Black shale deposition, atmospheric CO_2 drawdown, and cooling during the Cenomanian–Turonian oceanic anoxic event. *Paleoceanography, 26*(PA3201), 1–17.

Jati, M., Grosheny, D., Ferry, S., Masrour, M., Aoutem, M., Içame, N., et al. (2010). The Cenomanian–Turonian boundary event onthe Moroccan Atlantic margin (Agadir basin): Stable isotope and sequence stratigraphy. *Palaeogeography, Palaeoclimatology, Palaeoecology, 296,* 151–164.

Jefferies, R., & Milton, P. (1965). The mode of life of two Jurassic species of "Posidonia" (Bivalvia). *Palaeontology, 8,* 156–185.

Jenkyns, H. C. (1980). Cretaceous anoxic events: From continents to oceans. *Journal of the Geological Society, London, 137,* 171–188.

Jones, C. E., & Jenkyns, H. C. (2001). Seawater strontium isotopes, oceanic anoxic events, and seafloor hydrothermal activity in the Jurassic and Cretaceous. *American Journal of Science, 301,* 112–149.

Karakitsios, V., Tsikos, H., Van Breugel, Y., Koletti, L., Damste, J. S. S., & Jenkyns, H. C. (2007). First evidence for the Cenomanian–Turonian oceanic anoxic event (OAE2, 'Bonarelli' event) from the Ionian Zone, western continental Greece. *International Journal Earth Sciences, 96,* 343–352.

Keller, G., Berner, Z., Adatte, T., & Stueben, D. (2004). Cenomanian–Turonian and δ13C, and δ18O, sea level and salinity variations at Pueblo, Colorado. *Palaeogeography, Palaeoclimatology, Palaeoecology, 211,* 19–43.

Keller, G., Han, Q., Adatte, T., & Burns, S. (2001). Palaeoenvironment of the Cenomanian–Turonian transition at Eastbourne, England. *Cretaceous Research, 22,* 391–422.

Keller, G., & Pardo, A. (2004a). Age and paleoenvironment of the Cenomanian/Turonian global stratotype section and point at Pueblo, Colorado. *Marine Micropaleontology, 51,* 95–128.

Keller, G., & Pardo, A. (2004b). Disaster opportunists Guembelitrinidae: Index for environmental catastrophes. *Marine Micropaleontology, 53,* 83–116.

Kennedy, W. J., Walaszczyk, I., & Cobban, W. A. (2005). The global boundary stratotype section and point for the base of the Turonian stage of the Cretaceous: Pueblo, Colorado, USA. *Episodes, 28,* 93–104.

Kolonic, S., Wagner, T., Forster, A., Damste, J. S. S., Walsworth-Bell, B., Erba, E., et al. (2005). Black shale deposition on the northwest African Shelf during the Cenomanin/Turonian oceanic anoxic event: Climatic coumpling and global organic carbon burial. *Paleoceanography, 20,* PA1006. https://doi.org/10.1029/2003pa000950.

Kunht, W., Luderer, F., Nederbragt, S., Thurow, J., & Wagner, T. (2005). Orbital-scale record of the late Cenomanian–Turonian oceanic anoxic event (OAE-2) in the Tarfaya Basin (Morocco). *International Journal of Earth Sciences, 94,* 147–159.

Kuroda, J., Ogawa, N. O., Tanimizu, M., Coffin, M. T., Tokuyama, H., Kitazato, H., et al. (2007). Contemporaneous massive subaerial volcanism and late Cretaceous oceanic anoxic event 2. *Earth Planetary Science Letters, 256,* 211–223.

Leckie, R. M. (1985). Foraminifera of the Cenomanian–Turonian boundary interval, Greenhorn Formation, Rock Canyon Anticline, Pueblo, Colorado. In L. M. Pratt, E. G. Kauffman, & F. B. Zelt (Eds.), *Fine-grained deposits and biofacies of the Cretaceous Western Interior Seaway: Evidence of cyclic sedimentary processes, fieldtrip guidebook 4* (pp. 139–149). Tulsa: SEPM.

Leckie, R. M., Bralower, T. J., & Cashman, R. (2002). Oceanic anoxic events and plankton evolution: Biotic response to tectonic forcing during the mid-Cretaceous. *Paleoceanography, 17,* PA1041. https://doi.org/10.1029/2001pa000623.

Leckie, R. M., Schmidt, M. G., Finkelstein, D., & Yuretich, R. (1991). Paleoceanographic and paleoclimatic interpretations of the Mancos Shale (Upper Cretaceous), Black Mesa Basin, Arizona. In J. D. Nations & J. G. Eaton (Eds.), *Stratigraphy, depositional environments, and sedimentary tectonics of the western margin* (pp. 139–152). Boulder: Cretaceous Western Interior Seaway, Geological Society of America Special Paper.

Leckie, R. M., Yuretich, R. F., West, L. O. L., Finkelstein, D., & Schmidt, M. (1998). Paleoceanography of the southwestern Interior Sea during the time of the Cenomanian–Turonian boundary (late Cretaceous). *SEPM Concepts in Sedimentology and Paleontology, 6,* 101–126.

Lézin, C., Andreu, B., Ettachfini, M., Walleez, M.-J., Lebedel, V., & Meister, C. (2012). The upper Cenomanian–Lower Turonian of the Preafrican Trough, Morocco. *Sedimentary Geology, 245–246,* 1–16.

Lowery, C. M., Cunningham, R., Barrie, C. D., & Bralower, T. (2017). The Northern Gulf of Mexico during OAE2 and the relationship between water depth and black shale development. *Paleoceanography, 32,* 1316–1335.

Lowery, C. M., Leckie, R. M., Bryant, R., Elderbak, K., Parker, A., Polyak, D. E., et al. (2018). The Late Cretaceous Western Interior Seaway as a model for oxygenation change in epicontinental restricted basins. *Earth-Science Reviews, 177,* 545–564.

Luciani, V., & Cobianchi, M. (1999). The Bonarelli Level and other black shales in the Cenomanian–Turonian of the northeastern Dolomites (Italy): Calcareous nannofossil and foraminiferal data. *Cretaceous Research, 20,* 135–167.

Lüning, S., Kolonic, S., Belhadj, E. M., Belhadj, Z., Cota, L., Baric, G., et al. (2004). Integrated depositional model for the Cenomanian–Turonian organic-rich strata in North Africa. *Earth-Science Reviews, 64*, 51–117.

Lüning, S., Marzouk, A. M., Morsi, A. M., & Kuss, J. (1998). Sequence stratigraphy of the Upper Cretaceous of central-east Sinai, Egypt. *Cretaceous Research, 19*, 153–196.

Maamouri, A. L., Zaghbib-Turki, D., Matmati, M. F., Chikhaoui, M., & Salaj, J. (1994). La formation Bahloul en Tunisie centro-septentrionale: Variations latérales, nouvelle datation et nouvelle in-terprétation en terme de stratigraphie séquentielle. *Journal of African Earth Sciences, 18*, 37–50.

Meister, C., & Abdallah, H. (2005). Précision sur les successions d' ammonites du Cénomanien–Turonien dans la région de Gafsa, Tunisie du centre-sud. *Revue de Paléobiologie, 24*, 111–199.

Meister, C., Alzouma, K., Lang, J., & Mathey, B. (1992). Les ammonites du Niger et la transgression transsaharienne au cours du Cénomanien–Turonien. *Geobios, 25*, 55–100.

Meister, C., & Rhalmi, M. (2002). Quelques ammonites du Cénomanien–Turonien de la région d'Errachidia-Boudnid-Erfoud (partie méridionale du Haut Atlas Central, Maroc). *Revue de Paléobiologie, 21*, 759–779.

Monteiro, F. M., Pancost, R. D., Ridwell, A., & Donnadieu, Y. (2012). Nutrients as the dominant control on the spread of anoxia and euxinia across the Cenomanian–Turonian oceanic anoxic event (OAE2): Model-data comparison. *Paleoceanography, 27*, PA4209.

Moody, R. T. J., & Sutcliffe, P. J. C. (1991). The Cretaceous deposits of the Iullemmeden Basin of Niger, central West Africa. *Cretaceous Research, 12*, 137–157.

Mort, H., Jacquant, O., Adatte, T., Steinmann, P., Föllmi, K., Matera, V., et al. (2007). The Cenomanian/Turonian anoxic event at the Bonarelli level in Italy and Spain: Enhanced productivity and/or better preservation? *Cretaceous Research, 28*, 597–612.

Nagm, E. (2015). Stratigraphic significance of rapid faunal change across the Cenomanian–Turonian boundary in the Eastern Desert, Egypt. *Cretaceous Research, 52*, 9–24.

Naili, H., Belhadj, Z., Robaszynski, F., & Caron, M. (1995). Présence de roches mère à faciès Bahloul vers la limite Cénomanien–Turonien dans la région de Tébessa (Algérie orientale). *Notes du Service Géologique de Tunisie, 61*, 19–32.

Nederbragt, A. J., Erlich, R. N., Fouke, B. W., & Ganssen, G. M. (1998). Palaeoecology of the biserial planktonic foraminifer *Heterohelix moremani* (Cushman) in the late Albian to middle Turonian Circum-North Atlantic. *Palaeogeography, Palaeoclimatology, Palaeoecology, 144*, 115–133.

Nederbragt, A. J., & Fiorentino, A. (1999). Stratigraphy and paleoceanography of the Cenomanian–Turonian Boundary Event in Oued Mellegue, north-western Tunisia. *Cretaceous Research, 20*, 47–62.

Negra, M. H., Zagrarni, M. F., Hanini, A., & Strasser, A. (2011). The filament event near the Cenomanian–Turonian boundary in Tunisia: Filament origin and environmental signification. *Bulletin Société Géologique France, 182*, 507–519.

Norris, R. D., & Wilson, P. A. (1998). Low-latitude sea-surface temperature for the mid Cretaceous and the evolution of planktic foraminifera. *Geology, 26*, 823–826.

Okosun, E. A. (1992). Cretaceous ostracod biostratigraphy from Chad Bassin in Nigeria. *Journal of African Earth Sciences, 3*, 327–339.

Paul, C. R. C., & Lamolda, M. A. (2009). Testing the precision of bioevents. *Geological Magazine, 146*, 625–637.

Pavlishina, P., & Wagreich, M. (2012). Biostratigraphy and paleoenvironments in a northwestern TethyanCenomanian–Turonian boundary section (Austria) based on palynology and calcareous nannofossils. *Cretaceous Research, 38*, 103–112.

Pearce, C. R., Jarvis, I., & Tocher, B. A. (2009). The Cenomanian–Turonian boundary event, OAE 2 and palaeoenvironmental change in epicontinental seas: New insights from the dinocyst and geochemical records. *Palaeogeography, Palaeoclimatology, Palaeoecology, 280*, 207–234.

Peryt, D., & Wyrwicka, K. (1991). The Cenomanian–Turonian oceanic anoxic event in SE Poland. *Cretaceous Research, 12*, 65–80.

Poulsen, C. J., Barron, E. J., Arthur, M. A., & Peterson, W. H. (2001). Response of mid-Cretaceoys global oceanic circulation to tectonic and CO2 forcings. *Paleoceanography, 16*, 1–17.

Pratt, L. M., & Threlkeld, C. N. (1984). Stratigraphic significance of 13C/12C ratios in mid-Cretaceous rocks of the Western Interior, USA. In D. F. Slott & D. J. Glass (Eds.), *Mesozoic of middle North America* (Vol. 9, pp. 305–312). Calgary: Canadian Society of Petroleum Geologists Memoir.

Prauss, M. L. (2012). The Cenomanian/Turonian boundary event (CTBE) at Tarfaya, Morocco, northwest Africa: Eccentricity controlled water column stratification as major factor for total organic carbon (TOC) accumulation: Evidence from marine palynology. *Cretaceous Research, 37*, 246–260.

Price, G. D., & Hart, M. B. (2002). Isotopic evidence for early to mid-Cretaceous ocean temperature variability. *Marine Micropaleontology, 46*, 45–58.

Price, G. D., Sellwood, B., Corfield, R. M., Clarke, L. J., & Cartlidge, J. E. (1998). Isotopic evidence for paleotemperatures and depth stratification of middle Cretaceous planktonic foraminfiers from the Pacific Ocean. *Geological Magazine, 135*, 183–191.

Prokoph, A., Babalola, L. O., El Bilali, H., Olagoke, S., & Rachold, V. (2013). Cenomanian Turonian carbon isotope stratigraphy of the Western Canadian Sedimentary Basin. *Cretaceous Research, 44*, 39–53.

Reolid, M., Sánchez-Quiñónez, C. A., Alegret, L., & Molina, E. (2015). Palaeoenvironmental turnover across the Cenomanian–Turonian transition in Oued Bahloul, Tunisia: Foraminifera and geochemical proxies. *Palaeogeography, Palaeoclimatology, Palaeoecology, 417*, 491–510.

Reolid, M., Sánchez-Quiñónez, C. A., Alegret, L., & Molina, E. (2016). The biotic crisis across the oceanic anoxic event 2: Palaeoenvironmental inferences based on foraminifera and geochemical proxies from the South Iberian Palaeomargin. *Cretaceous Research, 60*, 1–27.

Rhalmi, M., Pascal, A., & Chellai, E. H. (2000). Litho-biostratigraphie, diagenèse et paléogéographie au Cénomanien supérieur–Turonien inférieur des bassins sud-atlasiques marocains. *Géologie Alpine, 76*, 135–149.

Robaszynski, F. (1989). L'événement à l'échelle gobale pendant la partie moyenne du Crétacé. *Geobios, Mémoire Spécial, 11*, 311–319.

Robaszynski, F., Amédro, F., & Caron, M. (1993a). La limite Cénomanien–Turonien et la Formation Bahloul dans quelques localités de Tunisie Centrale. *Cretaceous Research, 14*, 477–486.

Robaszynski, F., & Caron, M. (1995). Foraminifères planctoniques du Crétacé: Commentaire de la zonation Europe-Méditerranée. *Bulletin Société Géolologique de France, 166*, 681–692.

Robaszynski, F., Caron, M., Amédro, F., Dupuis, C., Hardenbol, J., Gonzalez Donoso, J. M., et al. (1993b). Le Cénomanien de la région de Kalaat Senan (Tunisie centrale): Litho-biostratigraphie et interprétation séquentielle. *Revue Micropaléontologie, 12*, 351–505.

Robaszynski, F., Caron, M., Amédro, F., Dupuis, C., Hardenbol, J., Gonzalez Donoso, J. M., et al. (1994). Le Cénomanien de la région de Kalaat Senan (Tunisie centrale). Litho-biostratigraphie et interprétation séquentielle. *Revue de Paléobiologie, 12*, 351–505.

Robaszynski, F., Caron, M., Dupuis, C., Amédro, F., Gonzalez-Dononso, J. M., Linares, D., et al. (1990). A tentative integrated

stratigraphy in the Turonian of Central Tunisia: Formations, zones and sequential stratigraphy in the Kalaat Senan area. *Bulletin des Centres de Recherche Exploration-Production Elf-Aquitaine, 14,* 218–384.

Robaszynski, F., Hardenbol, J., Caron, M., Amédro, F., Dupuis, C., Gonzalez-Dononso, J. M., et al. (1993c). Stratigraphie séquentielle dans un environnement distal: le Cénomanien de la région de Kalaat Senan (Tunisie Centrale). *Bulletin des Centres de Recherche Exploration-Production Elf-Aquitaine, 17,* 395–433.

Robaszynski, F., Zagrararni, M. F., Caron, M., & Amedro, F. (2010). The global bio-event at the Cenomanian–Turonien transition in the reduced Bahloul Formation of Bou Ghanem (central Tunisia). *Cretaceous Research, 31,* 1–15.

Ruault-Djerrab, M., Ferré, B., Kechid-Benkherouf, F., & Djerrab, A. (2012). Etude micropaléontologique du Cénomano-Turonien dans la région de Tébessa (NE Algérie): Implications paléoenvironnementales et recherche de l'empreinte de l'OAE2. *Revue de Paléobiologie, 31,* 127–144.

Ruault-Djerrab, M., Kechid-Benkherouf, F., & Djerrab, A. (2014). Données paléoenvironnementales sur le Vraconnien/Cénomanien de la région de Tébessa (Atlas Saharien, nord-est Algérie). Caractérisation de l'OAE2. *Annales de Paléontologie, 100,* 343–359.

Scaife, J. D., Ruhl, M., Dickson, A. J., Mather, T. A., Jenkyns, H. C., Percival, L. M. E., et al. (2017). Sedimentary mercury enrichments as a marker for submarine large igneous province volcanism? Evidence from the Mid-Cenomanian event and oceanic anoxic event 2 (Late Cretaceous). *Geochemistry, Geophysics, Geosystems, 18,* 4253–4275.

Schlanger, S. O., & Jenkyns, H. C. (1976). Cretaceoys oceanic anoxic events: Causes and consequences. *Geologie en Mijnbouw, 55,* 179–184.

Scopelliti, S. O., Bellanca, A., Coccioni, R., Luciani, V., Neri, R., Baudin, F., et al. (2004). High-resolution geochemical and biotic records of the Tethyan'Bonarelli Level' (OAE2, latest Cenomanian) from the Calabianca–Guidaloca composite section, north-western Sicily, Italy. *Palaeogeography, Palaeoclimatology, Palaeoecology, 208,* 293–317.

Scopelliti, G., Bellanca, A., Erba, E., Jenkyns, H. C., Neri, R., Tamagnini, P., et al. (2008). Cenomanian–Turonian carbonate and organic-carbon isotope records, biostratigraphy and provenance of a key section in NE Sicily, Italy: Palaeoceanographic and palaeogeographic implications. *Palaeogeography, Palaeoclimatology, Palaeoecology, 265,* 59–77.

Scotese, C. R. (2011). Paleogeographic and paleoclimatic atlas. Search and Discovery Article #30192. http://www.searchandd iscovery.com/pdfz/documents/2011/30192scotese/ndx_scote se.pdf.html. Accessed 28 Apr 2018.

Shahin, A. (1991). Cenomanian–Turonian ostracods from Gebel Nezzazat, southwestern Sinai, Egypt, with observations on δ13C values and the Cenomanian/Turonian boundary. *Journal of Micropalaeontology, 10,* 133–155.

Shahin, A. (2007). Oxygen and Carbon isotopes and foraminiferal biostratigraphy of the Cenomanian–Turonian succession in Gabal Nezzazat, southwestern Sinai, Egypt. *Revue de Paléobiologie, 26,* 359–379.

Shahin, A., & Elbaz, S. (2013). Cenomanian–Early Turonian of the shallow marine carbonate platform sequence at west central Sinai: Biostratigraphy, paleobathymetry and paleobiogeography. *Revue de Micropaléontologie, 56,* 103–126.

Smith, A. B., Gale, A. S., & Monks, N. E. A. (2001). Sea-level change and rock-record bias in the Cretaceous: A problem for extinction and biodiversity studies. *Paleobiology, 27,* 241–253.

Soua, M. (2011). Le Passage Cénomanien–Turonien en Tunisie: Biostratigraphie, chimiostratigraphie, cyclostratigraphie et stratigraphie séquentielle. Ph.D. Thesis Université de Tunis El Manar.

Soua, M. (2013). Siliceous and organic-rich sedimentation during the Cenomanian–Turonian oceanic anoxic event (OAE2) on the northern margin of Africa: An evidence from the Bargou area, Tunisia. *Arabian Journal of Geosciences, 6,* 1537–1557.

Soua, M., and Tribovillard, N. (2007). Depositional model at the Cenomanian/Turonian boundary for the Bahloul Formation, Tunisia. *Comptes Rendus Géoscience,* *339*(10), 692–701.

Soua, M., Zaghbib-Turki, D., & O'Dogherty, L. (2006). Les réponses biotiques des radiolaires à l'événement anoxique du Cénomanien supérieur dans la marge sud Téthysienne (Tunisie). *Mémoire ETAP, 26,* 195–216.

Soua, M., Zaghib-Turki, D., Fakhfakh-BenJemia, H., Smaoui, J., & Boukadi, A. (2011). The geochemical record of the Cenomanian–Turonian anoxic event in Tunisia. Is it correlative and isochronous to the biotic signal? *Acta Geologica Sinica, 85,* 801–840.

Takashima, R., Nishi, H., Hayashi, K., Okada, H., Kawahata, H., Yamanaka, T., et al. (2009). Litho-, bio- and chemostratigraphy across the Cenomanian/Turonian boundary (OAE 2) in the Vocontian Basin of southeastern France. *Palaeogeography, Palaeoclimatology, Palaeoecology, 273,* 61–74.

Topper, R. P. M., Trabucho-Alexandre, J., Tuenter, E., & Meijer, P. T. (2011). A regional ocean circulation model for the mid-Cretaceous North Atlantic Basin: Implications for black shale formation. *Climate of the Past, 7,* 277–297.

Trabucho-Alexandre, J., Tuenter, E., Henstra, G. A., van der Zwan, K. J., van de Wal, R. S. W., Dijkstra, H. A., et al. (2010). The mid-Cretaceous North Atlantic nutrient trap: Black shales and OAEs. *Paleoceanography, 25,* PA4201.

Tronchetti, G., & Grosheny, D. (1991). Les assemblages de foraminifères benthiques au passage Cénomanien–Turonien à Vergons, S-E France. *Geobios, 24,* 13–31.

Tsikos, H., Jenkyns, H. C., Walworth-Well, B., Petrizzo, M. R., Forster, A., Kolonic, S., et al. (2004). Carbon isotope stratigraphy recorded by the Cenomanian–Turonian oceanic anoxic event: Correlation and implications based on three key localities. *Journal of the Geological Society, 161,* 711–719.

Turgeon, S. C., & Creaser, R. A. (2008). Cretaceous oceanic anoxic event 2 triggered by a massive magmatic episode. *Nature, 454,* 323–326.

Uchman, A., Rodríguez-Tovar, F. J., & Oszczypko, N. (2013). Exceptionally favourable life conditions for macrobenthos during the Late Cenomanian OAE- 2 event: Ichnological record from the Bonarelli Level in the Grajcarek Unit, Polish Carpathians. *Cretaceous Research, 46,* 1–10.

Voigt, S., Erbacher, J., Mutterlose, J., Weiss, W., Westerhold, T., Wiese, F., et al. (2008). The Cenomanian–Turonian of the Wunstorf section—(North Germany): Global stratigraphic reference section and new orbital time scale for oceanic anoxic event 2. *Newsletters on Stratigraphy, 43,* 65–89.

Wanas, H. A. (2008). Cenomanian rocks in the Sinai Peninsula, Northeast Egypt: Facies analysis and sequence stratigraphy. *Journal of African Earth Sciences, 52,* 125–138.

Westermann, S., Caron, M., Fiet, N., Fleitmann, D., Matera, V., Adatte, T., et al. (2010). Evidence for oxic conditions during oceanic anoxic event 2 in the northern Tethyan pelagic realm. *Cretaceous Research, 31,* 500–514.

Wilmsen, M., & Nagm, E. (2013). Sequence stratigraphy of the lower Upper Cretaceous (Upper Cenomanian–Turonian) of the Eastern Desert, Egypt. *Newsletters on Stratigraphy, 46,* 23–46.

Wu, J., Liu, C., Fürsich, F. T., Yang, T., & Yin, J. (2015). Foraminifera as environmental indicators and quantitative salinity reconstructions in the Pearl River estuary, Southern China. *Journal of Foraminiferal Research, 45,* 205–219.

Yilmaz, I. O., Altiner, D., Tekin, U. K., Tuysuz, O., Faruk Ocakoglu, F., & Acikalin, S. (2010). Cenomanian–Turonian oceanic

anoxic event (OAE2) in the Sakarya Zone, northwestern Turkey: Sedimentological, cyclostratigraphic, and geochemical records. *Cretaceous Research, 31,* 207–226.

Zaghbib-Turki, D., & Soua, M. (2013). High resolution biostratigraphy of the Cenomanian–Turonian interval (OAE2) based on planktonic foraminiferal bioevents in North-Central Tunisia. *Journal of African Earth Sciences, 78,* 97–108.

Zagrarni, M. F., Negra, M. H., & Amine Hanini, A. (2008). Cenomanian–Turonian facies and sequence stratigraphy, Bahloul Formation, Tunisia. *Sedimentary Geology, 204,* 18–35.

Zaoui, D., Meister, C., Benyuocef, M., Bensalah, M., Piuz, A., Tchenar, S., et al. (2017). Cenomanian–Turonian ammonite successions in the Tinrhert Basin (Southeast Algeria): Revision and new data. *Cretaceous Research.* https://doi.org/10.1016/j.cretres.2017.09.011.

Affiliations

Mustapha Benadla[1] · Matías Reolid[2] · Abbas Marok[1] · Nezha El Kamali[3]

✉ Matías Reolid
mreolid@ujaen.es

Mustapha Benadla
benadla_mustapha@yahoo.fr

Abbas Marok
a_marok@yahoo.fr

Nezha El Kamali
elkamalinezha@yahoo.fr

[1] Department of Earth and Universe Sciences, University of Tlemcen, P.O. Box 119, Tlemcen, Algeria

[2] Departamento de Geología, Universidad de Jaén, Campus Las Lagunillas s/n, 23071 Jaén, Spain

[3] Faculté des Sciences, Université Ibn Zohr, Agadir, Morocco